

ENCLOSURE 7 TO AEP-NRC-2018-02

WCAP-18295-NP, Revision 0 "Technical Justification for Eliminating Accumulator Line Rupture as the Structural Design Basis for D.C. Cook Units 1 and 2, Using Leak-Before-Break Methodology" (Non-Proprietary)

**Technical Justification for
Eliminating Accumulator Line
Rupture as the Structural Design
Basis for D.C. Cook Units 1 and 2,
Using Leak-Before-Break
Methodology**



WCAP-18295-NP
Revision 0

**Technical Justification for Eliminating
Accumulator Line Rupture as the Structural Design Basis
for D.C. Cook Units 1 and 2,
Using Leak-Before-Break Methodology**

January 2018

Author: Christopher R. Kirby*
Structural Design and Analysis - I

Reviewer: Eric D. Johnson*
Structural Design and Analysis - II

Approved: Benjamin A. Leber, Manager*
Structural Design and Analysis - II

*Electronically approved records are authenticated in the electronic document management system.

Westinghouse Electric Company LLC
1000 Westinghouse Drive
Cranberry Township, PA 16066, USA

© 2018 Westinghouse Electric Company LLC
All Rights Reserved

TABLE OF CONTENTS

1.0	Introduction.....	1-1
1.1	Purpose	1-1
1.2	Scope and Objectives.....	1-1
1.3	References.....	1-2
2.0	Operation and Stability of the Reactor Coolant System	2-1
2.1	Stress Corrosion Cracking	2-1
2.2	Water Hammer	2-2
2.3	Low Cycle and High Cycle Fatigue.....	2-2
2.4	Other Possible Degradation During Service of the Accumulator Lines	2-3
2.5	References.....	2-3
3.0	Pipe Geometry and Loading	3-1
3.1	Calculations of Loads and Stresses.....	3-1
3.2	Loads for Leak Rate Evaluation	3-1
3.3	Load Combination for Crack Stability Analyses	3-2
3.4	References.....	3-3
4.0	Material Characterization.....	4-1
4.1	Accumulator Line Pipe Material and Weld Process	4-1
4.2	Tensile Properties.....	4-1
4.3	Reference	4-1
5.0	Critical Locations.....	5-1
5.1	Critical Locations.....	5-1
6.0	Leak Rate Predictions	6-1
6.1	Introduction.....	6-1
6.2	General Considerations.....	6-1
6.3	Calculation Method.....	6-1
6.4	Leak Rate Calculations	6-2
6.5	References.....	6-3
7.0	Fracture Mechanics Evaluation.....	7-1
7.1	Global Failure Mechanism.....	7-1
7.2	Local Failure Mechanism	7-2
7.3	Results of Crack Stability Evaluation	7-2
7.4	References.....	7-2
8.0	Assessment of Fatigue Crack Growth.....	8-1
8.1	References.....	8-1
9.0	Assessment of Margins	9-1
10.0	Conclusions.....	10-1
	Appendix A: Limit Moment.....	A-1

LIST OF TABLES

Table 3-1	Summary of D.C. Cook Unit 1 Piping Geometry and Normal Operating Condition for 10-inch Accumulator Lines	3-4
Table 3-2	Summary of D.C. Cook Unit 2 Piping Geometry and Normal Operating Condition for 10-inch Accumulator Lines	3-5
Table 3-3	Summary of D.C. Cook Unit 1 Normal Loads and Stresses for 10-inch Accumulator Injection Line Loop 1.....	3-6
Table 3-4	Summary of D.C. Cook Unit 1 Normal Loads and Stresses for 10-inch Accumulator Injection Line Loop 2.....	3-7
Table 3-5	Summary of D.C. Cook Unit 1 Normal Loads and Stresses for 10-inch Accumulator Injection Line Loop 3.....	3-8
Table 3-6	Summary of D.C. Cook Unit 1 Normal Loads and Stresses for 10-inch Accumulator Injection Line Loop 4.....	3-9
Table 3-7	Summary of D.C. Cook Unit 2 Normal Loads and Stresses for 10-inch Accumulator Injection Line Loop 1.....	3-10
Table 3-8	Summary of D.C. Cook Unit 2 Normal Loads and Stresses for 10-inch Accumulator Injection Line Loop 2.....	3-11
Table 3-9	Summary of D.C. Cook Unit 2 Normal Loads and Stresses for 10-inch Accumulator Injection Line Loop 3.....	3-12
Table 3-10	Summary of D.C. Cook Unit 2 Normal Loads and Stresses for 10-inch Accumulator Injection Line Loop 4.....	3-13
Table 3-11	Summary of D.C. Cook Unit 1 Faulted Loads and Stresses for 10-inch Accumulator Injection Line Loop 1.....	3-14
Table 3-12	Summary of D.C. Cook Unit 1 Faulted Loads and Stresses for 10-inch Accumulator Injection Line Loop 2.....	3-15
Table 3-13	Summary of D.C. Cook Unit 1 Faulted Loads and Stresses for 10-inch Accumulator Injection Line Loop 3.....	3-16
Table 3-14	Summary of D.C. Cook Unit 1 Faulted Loads and Stresses for 10-inch Accumulator Injection Line Loop 4.....	3-17
Table 3-15	Summary of D.C. Cook Unit 2 Faulted Loads and Stresses for 10-inch Accumulator Injection Line Loop 1.....	3-18
Table 3-16	Summary of D.C. Cook Unit 2 Faulted Loads and Stresses for 10-inch Accumulator Injection Line Loop 2.....	3-19
Table 3-17	Summary of D.C. Cook Unit 2 Faulted Loads and Stresses for 10-inch Accumulator Injection Line Loop 3.....	3-20

Table 3-18	Summary of D.C. Cook Unit 2 Faulted Loads and Stresses for 10-inch Accumulator Injection Line Loop 4.....	3-21
Table 4-1	Mechanical Properties for 10-inch Accumulator Lines Material at Operating Temperatures for D.C. Cook Units 1 and 2.....	4-1
Table 5-1	Summary of D.C. Cook Unit 1 Piping Geometry and Normal Operating Condition for 10-inch Accumulator Lines and Critical Locations.....	5-1
Table 6-1	Flaw Sizes Yielding a Leak Rate of 8 gpm for the D.C. Cook Unit 1 and 2 10-inch Accumulator Lines	6-3
Table 7-1	Stability Results for the D.C. Cook Unit 1 and 2 10-inch Accumulator Lines Based on Limit Load.....	7-3
Table 9-1	Leakage Flaw Sizes, Critical Flaw Sizes and Margins for D.C. Cook Units 1 and 2 10-inch Accumulator Lines.....	9-1

LIST OF FIGURES

Figure 3-1	10-inch Accumulator Line Layout Showing Segments for D.C. Cook Units 1 and 2.....	3-22
Figure 3-2	D.C. Cook Unit 1 Accumulator Line Loop 1 Layout Showing Weld Locations with Node Points.....	3-23
Figure 3-3	D.C. Cook Unit 1 Accumulator Line Loop 2 Layout Showing Weld Locations with Node Points.....	3-24
Figure 3-4	D.C. Cook Unit 1 Accumulator Line Loop 3 Layout Showing Weld Locations with Node Points.....	3-25
Figure 3-5	D.C. Cook Unit 1 Accumulator Line Loop 4 Layout Showing Weld Locations with Node Points.....	3-26
Figure 3-6	D.C. Cook Unit 2 Accumulator Line Loop 1 Layout Showing Weld Locations with Node Points.....	3-27
Figure 3-7	D.C. Cook Unit 2 Accumulator Line Loop 2 Layout Showing Weld Locations with Node Points.....	3-28
Figure 3-8	D.C. Cook Unit 2 Accumulator Line Loop 3 Layout Showing Weld Locations with Node Points.....	3-29
Figure 3-9	D.C. Cook Unit 2 Accumulator Line Loop 4 Layout Showing Weld Locations with Node Points.....	3-30
Figure 5-1	Layout Showing Critical Location Loop 4 Unit 2	5-2
Figure 5-2	Layout Showing Critical Locations Loop 3 Unit 2.....	5-3
Figure 5-3	Layout Showing Critical Locations Loop 1 Unit 2.....	5-4
Figure 6-1	Analytical Predictions of Critical Flow Rates of Steam-Water Mixtures	6-4
Figure 6-2	[σ] ^{a,c,e} Pressure Ratio as a Function of L/D.....	6-5
Figure 6-3	Idealized Pressure Drop Profile Through a Postulated Crack.....	6-6
Figure 7-1	[σ] ^{a,c,e} Stress Distribution	7-4
Figure A-1	Pipe with a Through-Wall Crack in Bending.....	A-2

1.0 INTRODUCTION

1.1 PURPOSE

The current structural design basis for the D.C. Cook Units 1 and 2 10-inch accumulator lines (from the cold legs Loop 1, Loop 2, Loop 3 and Loop 4) require postulating non-mechanistic circumferential and longitudinal pipe breaks. This results in additional plant hardware (e.g., pipe whip restraints and jet shields) which would mitigate the dynamic consequences of the pipe breaks. It is, therefore, highly desirable to be realistic in the postulation of pipe breaks for the accumulator lines. Presented in this report are the descriptions of a mechanistic pipe break evaluation method and the analytical results that can be used for establishing that a circumferential type of break will not occur within the accumulator lines. The evaluations consider that circumferentially oriented flaws cover longitudinal cases.

1.2 SCOPE AND OBJECTIVES

The purpose of this investigation is to demonstrate Leak Before Break (LBB) for the D.C. Cook Units 1 and 2 accumulator lines from the cold legs Loop 1, Loop 2, Loop 3 and Loop 4 to the isolation valves near the accumulator tanks. Schematic drawings of the piping system are shown in Section 3.0. The recommendations and criteria proposed in SRP 3.6.3 (References 1-1 and 1-2) are used in this evaluation. The criteria and the resulting steps of the evaluation procedure can be briefly summarized as follows:

1. Calculate the applied loads based on as-built configuration. Identify the location(s) at which the highest faulted stress occurs.
2. Identify the materials and the material properties.
3. Postulate a through-wall flaw at the governing location(s). The size of the flaw should be large enough so that the leakage is assured of detection with margin using the installed leak detection equipment when the pipe is subjected to normal operating loads. Demonstrate that there is a margin of 10 between the calculated leak rate and the leak detection capability.
4. Using maximum faulted loads in the stability analysis, demonstrate that there is a margin of 2 between the leakage size flaw and the critical size flaw.
5. Review the operating history to ascertain that operating experience has indicated no particular susceptibility to failure from the effects of corrosion, water hammer, or low and high cycle fatigue.
6. For the material types used in the plant, provide representative material properties.
7. Demonstrate margin on applied load by combining the faulted loads by absolute summation method.

This report provides a fracture mechanics demonstration of accumulator line piping integrity for D.C. Cook Units 1 and 2 consistent with the NRC's position for exemption from consideration of dynamic effects (Reference 1-3).

It should be noted that the terms “flaw” and “crack” have the same meaning and are used interchangeably. “Governing location” and “critical location” are also used interchangeably throughout the report.

1.3 REFERENCES

- 1-1 Standard Review Plan: Public Comments Solicited; 3.6.3 Leak-Before-Break Evaluation Procedures; Federal Register/Vol. 52, No. 167/Friday August 28, 1987/Notices, pp. 32626-32633.
- 1-2 NUREG-0800 Revision 1, March 2007, Standard Review Plan: 3.6.3 Leak-Before-Break Evaluation Procedures.
- 1-3 Nuclear Regulatory Commission, 10 CFR 50, Modification of General Design Criteria 4 Requirements for Protection Against Dynamic Effects of Postulated Pipe Ruptures, Final Rule, Federal Register/Vol. 52, No. 207/Tuesday, October 27, 1987/Rules and Regulations, pp. 41288-41295.

2.0 OPERATION AND STABILITY OF THE REACTOR COOLANT SYSTEM

2.1 STRESS CORROSION CRACKING

The Westinghouse reactor coolant system primary loops and connected Class 1 piping have an operating history that demonstrates the inherent operating stability characteristics of the design. This includes a low susceptibility to cracking failure from the effects of corrosion (e.g., intergranular stress corrosion cracking (IGSCC)). This operating history totals over 1400 reactor-years, including 16 plants each having over 30 years of operation, 10 other plants each with over 25 years of operation, 11 plants each with over 20 years of operation and 12 plants each with over 15 years of operation.

In 1978, the United States Nuclear Regulatory Commission (USNRC) formed the second Pipe Crack Study Group. (The first Pipe Crack Study Group (PCSG) established in 1975 addressed cracking in boiling water reactors only.) One of the objectives of the second PCSG was to include a review of the potential for stress corrosion cracking in Pressurized Water Reactors (PWRs). The results of the study performed by the PCSG were presented in NUREG-0531 (Reference 2-1) entitled "Investigation and Evaluation of Stress Corrosion Cracking in Piping of Light Water Reactor Plants." In that report the PCSG stated:

"The PCSG has determined that the potential for stress-corrosion cracking in PWR primary system piping is extremely low because the ingredients that produce IGSCC are not all present. The use of hydrazine additives and a hydrogen overpressure limit the oxygen in the coolant to very low levels. Other impurities that might cause stress-corrosion cracking, such as halides or caustic, are also rigidly controlled. Only for brief periods during reactor shutdown when the coolant is exposed to the air and during the subsequent startup are conditions even marginally capable of producing stress-corrosion cracking in the primary systems of PWRs. Operating experience in PWRs supports this determination. To date, no stress corrosion cracking has been reported in the primary piping or safe ends of any PWR."

For stress corrosion cracking (SCC) to occur in piping, the following three conditions must exist simultaneously: high tensile stresses, susceptible material, and a corrosive environment. Since some residual stresses and some degree of material susceptibility exist in any stainless steel piping, the potential for stress corrosion is minimized by properly selecting a material immune to SCC as well as preventing the occurrence of a corrosive environment. The material specifications consider compatibility with the system's operating environment (both internal and external) as well as other material in the system, applicable ASME Code rules, fracture toughness, welding, fabrication, and processing.

The elements of a water environment known to increase the susceptibility of austenitic stainless steel to stress corrosion are: oxygen, fluorides, chlorides, hydroxides, hydrogen peroxide, and reduced forms of sulfur (e.g., sulfides, sulfites, and thionates). Strict pipe cleaning standards prior to operation and careful control of water chemistry during plant operation are used to prevent the occurrence of a corrosive environment. Prior to being put into service, the piping is cleaned internally and externally. During flushes and preoperational testing, water chemistry is controlled in accordance with written specifications.

Requirements on chlorides, fluorides, conductivity, and pH are included in the acceptance criteria for the piping.

During plant operation, the reactor coolant water chemistry is monitored and maintained within very specific limits. Contaminant concentrations are kept below the thresholds known to be conducive to stress corrosion cracking with the major water chemistry control standards being included in the plant operating procedures as a condition for plant operation. For example, during normal power operation, oxygen concentration in the RCS is expected to be in the parts per billion (ppb) range by controlling charging flow chemistry and maintaining hydrogen in the reactor coolant at specified concentrations. Halogen concentrations are also stringently controlled by maintaining concentrations of chlorides and fluorides within the specified limits. Thus during plant operation, the likelihood of stress corrosion cracking is minimized.

During 1979, several instances of cracking in PWR feedwater piping led to the establishment of the third PCSCG. The investigations of the PCSCG reported in NUREG-0691 (Reference 2-2) further confirmed that no occurrences of IGSCC have been reported for PWR primary coolant systems.

Primary Water Stress Corrosion Cracking (PWSCC) occurred in V. C. Summer reactor vessel hot leg nozzle, Alloy 82/182 weld. It should be noted that this susceptible material is not found in the D.C. Cook Unit 1 and 2 accumulator lines.

2.2 WATER HAMMER

Overall, there is a low potential for water hammer in the RCS and connecting accumulator lines since they are designed and operated to preclude the voiding condition in normally filled lines. The RCS and connecting accumulator lines including piping and components are designed for normal, upset, emergency, and faulted condition transients. The design requirements are conservative relative to both the number of transients and their severity. Relief valve actuation and the associated hydraulic transients following valve opening are considered in the system design. Other valve and pump actuations are relatively slow transients with no significant effect on the system dynamic loads. To ensure dynamic system stability, reactor coolant parameters are stringently controlled. Temperature during normal operation is maintained within a narrow range by the control rod positions; pressure is controlled also within a narrow range for steady-state conditions by the pressurizer heaters and pressurizer spray. The flow characteristics of the system remain constant during a fuel cycle because the only governing parameters, namely system resistance and the reactor coolant pump characteristics are controlled in the design process. Additionally, Westinghouse has instrumented typical reactor coolant systems to verify the flow and vibration characteristics of the system and the connecting auxiliary lines. Preoperational testing and operating experience has verified the Westinghouse approach. The operating transients of the RCS primary piping and connected accumulator lines are such that no significant water hammer can occur.

2.3 LOW CYCLE AND HIGH CYCLE FATIGUE

The 1967 Edition of the B31.1 Code does not contain an explicit piping low cycle fatigue analysis requirement. The B31.1 piping complies with a stress range reduction factor to be applied to the allowable stress as a way to address fatigue from full temperature cycles for thermal expansion stress evaluation. The stress range reduction factor is 1.0 (i.e., no reduction) for equivalent full temperature

cycles less than 7000. For D.C. Cook Units 1 and 2, the equivalent full temperature cycles for the applicable design transients are less than 7000, so no reduction is required.

Pump vibrations during operation would result in high cycle fatigue loads in the piping system. During operation, an alarm signals the exceedance of the RC pump shaft vibration limits. Field vibration measurements have been made on the reactor coolant loop piping in a number of plants during hot functional testing. Stresses in the elbow below the RC pump have been found analytically to be very small, between 2 and 3 ksi at the highest. Field measurements on typical PWR plant indicate vibration stress amplitudes less than 1 ksi. When translated to the connecting accumulator lines, these stresses would be even lower, well below the fatigue endurance limit for the accumulator line materials and would result in an applied stress intensity factor below the threshold for fatigue crack growth.

2.4 OTHER POSSIBLE DEGRADATION DURING SERVICE OF THE ACCUMULATOR LINES

The accumulator lines and the associated fittings for D.C. Cook Nuclear Power Plants are forged product forms, which are not susceptible to toughness degradation due to thermal aging.

The maximum normal operating temperature of the accumulator piping is about 549°F. This is well below the temperature that would cause any creep damage in stainless steel piping. Cleavage type failures are not a concern for the operating temperatures and the material used in the stainless steel piping of the accumulator lines.

Wall thinning by erosion and erosion-corrosion effects should not occur in the accumulator piping due to the low velocity, typically less than 1.0 ft/sec and the stainless steel material, which is highly resistant to these degradation mechanisms. Per NUREG-0691 (Reference 2-2), a study on pipe cracking in PWR piping reported only two incidents of wall thinning in stainless steel pipe and these were not in the accumulator line. The cause of wall thinning is related to the high water velocity and is therefore clearly not a mechanism that would affect the accumulator piping.

Brittle fracture for stainless steel material occurs when the operating temperature is about -200°F. Accumulator line operating temperature is higher than 120°F and therefore, brittle fracture is not a concern for the accumulator line.

2.5 REFERENCES

- 2-1 Investigation and Evaluation of Stress-Corrosion Cracking in Piping of Light Water Reactor Plants, NUREG-0531, U.S. Nuclear Regulatory Commission, February 1979.
- 2-2 Investigation and Evaluation of Cracking Incidents in Piping in Pressurized Water Reactors, NUREG-0691, U.S. Nuclear Regulatory Commission, September 1980.

3.0 PIPE GEOMETRY AND LOADING

3.1 CALCULATIONS OF LOADS AND STRESSES

The stresses due to axial loads and bending moments are calculated by the following equation:

$$\sigma = \frac{F}{A} + \frac{M}{Z} \quad (3-1)$$

where,

- σ = stress (psi)
- F = axial load (lbs)
- M = moment (in-lb)
- A = pipe cross-sectional area (in²)
- Z = section modulus (in³)

The moments for the desired loading combinations are calculated by the following equation:

$$M = \sqrt{M_x^2 + M_y^2 + M_z^2} \quad (3-2)$$

where,

- M_x = X component of moment, Torsion
- M_y = Y component of bending moment
- M_z = Z component of bending moment

The axial load and moments for leak rate predictions and crack stability analyses are computed by the methods to be explained in Sections 3.2 and 3.3.

3.2 LOADS FOR LEAK RATE EVALUATION

The normal operating loads for leak rate predictions are calculated by the following equations:

$$F = F_{DW} + F_{TH} + F_P \quad (3-3)$$

$$M_X = (M_X)_{DW} + (M_X)_{TH} \quad (3-4)$$

$$M_Y = (M_Y)_{DW} + (M_Y)_{TH} \quad (3-5)$$

$$M_Z = (M_Z)_{DW} + (M_Z)_{TH} \quad (3-6)$$

The subscripts of the above equations represent the following loading cases:

DW	=	deadweight
TH	=	normal thermal expansion
P	=	load due to internal pressure

This method of combining loads is often referred to as the algebraic sum method (References 3-1 and 3-2). The LBB evaluations do not include moment effects due to pressure loading since the moment loading is significantly dominated by the thermal loads for normal operation and by the seismic loads for faulted events.

The dimensions and normal operating conditions are given in Tables 3-1 and 3-2. The loads based on this method of combination are provided in Tables 3-3 to 3-10 at all the weld locations. The weld naming convention used in this report is as follows:

Unit # - Isometric # - Spool Sheet # - Analysis Node #

3.3 LOAD COMBINATION FOR CRACK STABILITY ANALYSES

In accordance with Standard Review Plan 3.6.3 (References 3-1 and 3-2), the absolute sum of loading components can be applied which results in higher magnitude of combined loads. If crack stability is demonstrated using these loads, the LBB margin on loads can be reduced from $\sqrt{2}$ to 1.0. The absolute summation of loads is shown in the following equations:

$$F = |F_{DW}| + |F_{TH}| + |F_P| + |F_{SSEINERTIA}| + |F_{SSEAM}| \quad (3-7)$$

$$M_X = |(M_X)_{DW}| + |(M_X)_{TH}| + |(M_X)_{SSEINERTIA}| + |(M_X)_{SSEAM}| \quad (3-8)$$

$$M_Y = |(M_Y)_{DW}| + |(M_Y)_{TH}| + |(M_Y)_{SSEINERTIA}| + |(M_Y)_{SSEAM}| \quad (3-9)$$

$$M_Z = |(M_Z)_{DW}| + |(M_Z)_{TH}| + |(M_Z)_{SSEINERTIA}| + |(M_Z)_{SSEAM}| \quad (3-10)$$

where subscript SSEINERTIA refers to safe shutdown earthquake inertia, SSEAM is safe shutdown earthquake anchor motion. It is noted that the D.C. Cook piping analyses consider Design Basis Earthquake (DBE) as the seismic criteria, which is equivalent to Safe Shutdown Earthquake (SSE).

The loads so determined are used in the fracture mechanics evaluations (Section 7.0) to demonstrate the LBB margins at the locations established to be the governing locations. These loads at all the weld locations are given in Tables 3-11 to 3-18.

Notes: For the accumulator lines, the LBB analysis will not be performed at the locations after the isolation valve near the accumulator tank since any break after the isolation valve will not have any effect on the primary loop piping system since there are two check valves, and the one isolation valve will

prevent the break propagation to the primary loop piping system. Figure 3-1 shows typical 10-inch accumulator line layout showing segments for D.C. Cook Units 1 and 2.

3.4 REFERENCES

- 3-1 Standard Review Plan: Public Comments Solicited; 3.6.3 Leak-Before-Break Evaluation Procedures; Federal Register/Vol. 52, No. 167/Friday, August 28, 1987/Notices, pp. 32626-32633.
- 3-2 NUREG-0800 Revision 1, March 2007, Standard Review Plan: 3.6.3 Leak-Before-Break Evaluation Procedures.

Table 3-1 Summary of D.C. Cook Unit 1 Piping Geometry and Normal Operating Condition for 10-inch Accumulator Lines							
Loop	Segment	Nodes	Material Type	Pipe Size & Schedule	Minimum Wall Thickness (in)	Normal Operating	
						Pressure (psig)	Temperature (°F)
1	I	416 to 412	A376 TP316 or A403 WP316	10-inch Sch. 140	0.896	2345	549
	II	406-404	A376 TP316 or A403 WP316	10-inch Sch. 140	0.896	2235	549
		404 to 450	A376 TP316 or A403 WP316	10-inch Sch. 140	0.896	2235	120
	III	456 to 459	A376 TP316 or A403 WP316	10-inch Sch. 140	0.896	644	120
2	I	361 to 358	A376 TP316 or A403 WP316	10-inch Sch. 140	0.896	2345	549
	II	352 to 350	A376 TP316 or A403 WP316	10-inch Sch. 140	0.896	2235	549
		350 to 365	A376 TP316 or A403 WP316	10-inch Sch. 140	0.896	2235	120
	III	368 to 374	A376 TP316 or A403 WP316	10-inch Sch. 140	0.896	644	120
3	I	171 to 168	A376 TP316 or A403 WP316	10-inch Sch. 140	0.896	2345	549
	II	162 to 160	A376 TP316 or A403 WP316	10-inch Sch. 140	0.896	2235	549
		160 to 200	A376 TP316 or A403 WP316	10-inch Sch. 140	0.896	2235	120
	III	206 to 214	A376 TP316 or A403 WP316	10-inch Sch. 140	0.896	644	120
4	I	307 to 304	A376 TP316 or A403 WP316	10-inch Sch. 140	0.896	2345	549
	II	296 to 294	A376 TP316 or A403 WP316	10-inch Sch. 140	0.896	2235	549
		294 to 334	A376 TP316 or A403 WP316	10-inch Sch. 140	0.896	2235	120
	III	340 to 344	A376 TP316 or A403 WP316	10-inch Sch. 140	0.896	644	120

Notes: Pipe Outer Diameter = 10.75 in. Figure 3-1 shows the Segments. Node numbers are shown in Tables 3-3 to 3-6, Tables 3-11 to 3-14, and Figures 3-2 to 3-5.

The minimum wall thickness is conservatively based at the weld counterbore and not per ASME Code requirement.

Table 3-2 Summary of D.C. Cook Unit 2 Piping Geometry and Normal Operating Condition for 10-inch Accumulator Lines							
Loop	Segment	Nodes	Material Type	Pipe Size & Schedule	Minimum Wall Thickness (in)	Normal Operating	
						Pressure (psig)	Temperature (°F)
1	I	416 to 412	A376 TP316 or A403 WP316	10-inch Sch. 140	0.896	2345	549
	II	406-404	A376 TP316 or A403 WP316	10-inch Sch. 140	0.896	2235	549
		404 to 450	A376 TP316 or A403 WP316	10-inch Sch. 140	0.896	2235	120
	III	456 to 460	A376 TP316 or A403 WP316	10-inch Sch. 140	0.896	644	120
2	I	361 to 358	A376 TP316 or A403 WP316	10-inch Sch. 140	0.896	2345	549
	II	352 to 350	A376 TP316 or A403 WP316	10-inch Sch. 140	0.896	2235	549
		350 to 365	A376 TP316 or A403 WP316	10-inch Sch. 140	0.896	2235	120
	III	368 to 374	A376 TP316 or A403 WP316	10-inch Sch. 140	0.896	644	120
3	I	171 to 168	A376 TP316 or A403 WP316	10-inch Sch. 140	0.896	2345	549
	II	162 to 160	A376 TP316 or A403 WP316	10-inch Sch. 140	0.896	2235	549
		160 to 200	A376 TP316 or A403 WP316	10-inch Sch. 140	0.896	2235	120
	III	206 to 214	A376 TP316 or A403 WP316	10-inch Sch. 140	0.896	644	120
4	I	307 to 304	A376 TP316 or A403 WP316	10-inch Sch. 140	0.896	2345	549
	II	296 to 294	A376 TP316 or A403 WP316	10-inch Sch. 140	0.896	2235	549
		294 to 334	A376 TP316 or A403 WP316	10-inch Sch. 140	0.896	2235	120
	III	340 to 344	A376 TP316 or A403 WP316	10-inch Sch. 140	0.896	644	120

Notes: Pipe Outer Diameter = 10.75 in. Figure 3-1 shows the Segments. Node numbers are shown in Tables 3-7 to 3-10, Tables 3-15 to 3-18, and Figures 3-6 to 3-9.

The minimum wall thickness is conservatively based at the weld counterbore and not per ASME Code requirement.

Table 3-3 Summary of D.C. Cook Unit 1 Normal Loads and Stresses for 10-inch Accumulator Injection Line Loop 1			
Weld Location Node	Axial Force (lbs)	Moment (in-lbs)	Total Stress (psi)
1-SI-29-4-416	150,544	572,540	14,500
1-SI-29-4-412	151,904	480,244	13,087
1-SI-29-3R-406	144,981	372,401	11,129
1-SI-29-3R-404Y	144,974	359,707	10,927
1-SI-29-3R-404Z	144,603	329,751	10,439
1-SI-29-3R-420N	145,021	138,676	7,428
1-SI-29-3R-420F	132,866	302,148	9,579
1-SI-29-2-426N	132,866	610,416	14,462
1-SI-29-2-426F	135,542	584,316	14,145
1-SI-29-2-428N	135,361	511,059	12,978
1-SI-29-2-428F	134,368	418,866	11,482
1-SI-29-2-430N	133,973	187,196	7,798
1-SI-29-2-430F	134,456	217,782	8,300
1-SI-29-2-434N	133,786	596,012	14,267
1-SI-29-1-434F	132,348	606,825	14,386
1-SI-29-1-442N	140,744	19,109	5,379
1-SI-29-1-446F	144,828	24,490	5,612
1-SI-29-1-450	144,385	36,111	5,780
1-SI-28-1-456	42,094	48,043	2,279
1-SI-28-1-459	40,082	75,149	2,636

Notes:

- See Figure 3-2
- Axial force includes pressure

Weld Location Node	Axial Force (lbs)	Moment (in-lbs)	Total Stress (psi)
1-SI-31-4-361	150,050	553,834	14,186
1-SI-31-4-358	150,454	464,800	12,790
1-SI-31-3R-352	143,522	360,126	10,882
1-SI-31-3R-350X	143,515	349,881	10,719
1-SI-31-3R-350Z	137,879	329,396	10,191
1-SI-31-3R-348F	137,317	146,068	7,267
1-SI-31-3R-348N	148,662	305,946	10,209
1-SI-31-3R-344F	148,661	583,194	14,601
1-SI-31-2-344N	145,839	543,364	13,868
1-SI-31-2-342F	146,048	429,755	12,076
1-SI-31-2-342N	146,006	341,910	10,683
1-SI-31-2-340F	146,140	228,057	8,884
1-SI-31-2-340N	146,570	173,557	8,036
1-SI-31-1A-338F	147,466	601,975	14,855
1-SI-31-1A-338N	148,841	616,807	15,139
1-SI-31-1A-332F	141,852	49,529	5,901
1-SI-31-1A-332N	140,753	34,468	5,623
1-SI-31-1A-330F	140,754	34,318	5,621
1-SI-31-1A-324	141,694	60,896	6,076
1-SI-31-1A-324Y	144,566	42,505	5,888
1-SI-31-1A-365	144,181	38,709	5,814
1-SI-30-1-369N	41,878	33,833	2,046
1-SI-30-1-372F	40,592	43,134	2,147
1-SI-30-1-374	40,592	56,445	2,358

Notes:

- See Figure 3-3
- Axial force includes pressure

Table 3-5 Summary of D.C. Cook Unit 1 Normal Loads and Stresses for 10-inch Accumulator Injection Line Loop 3			
Weld Location Node	Axial Force (lbs)	Moment (in-lbs)	Total Stress (psi)
1-SI-33-4-171	149,402	545,932	14,037
1-SI-33-4-168	149,924	457,435	12,654
1-SI-33-3R-162	142,990	350,539	10,711
1-SI-33-3R-160Y	142,990	339,778	10,540
1-SI-33-3R-160Z	144,283	320,142	10,276
1-SI-33-3R-174N	144,756	159,702	7,751
1-SI-33-3R-174F	132,912	329,603	10,015
1-SI-33-3R-178N	132,912	587,067	14,094
1-SI-33-2-178F	135,855	544,167	13,520
1-SI-33-2-180N	135,647	426,577	11,650
1-SI-33-2-180F	135,829	337,504	10,246
1-SI-33-2-182N	135,715	250,216	8,859
1-SI-33-2-182F	135,186	188,126	7,856
1-SI-33-2-184N	134,254	625,921	14,758
1-SI-33-1A-184F	132,807	642,494	14,968
1-SI-33-1A-190N	140,752	82,640	6,386
1-SI-33-1A-196	140,684	98,910	6,641
1-SI-33-1A-196Y	143,247	91,767	6,621
1-SI-33-1A-200	142,911	82,455	6,461
1-SI-32-1-206	40,580	111,590	3,231
1-SI-32-1-214	38,140	133,951	3,498

Notes:

- See Figure 3-4
- Axial force includes pressure

Table 3-6 Summary of D.C. Cook Unit 1 Normal Loads and Stresses for 10-inch Accumulator Injection Line Loop 4			
Weld Location Node	Axial Force (lbs)	Moment (in-lbs)	Total Stress (psi)
1-SI-35-4-307	149,603	558,147	14,238
1-SI-35-4-304	150,581	465,700	12,809
1-SI-35-3RR-296	143,647	361,774	10,912
1-SI-35-3RR-294Y	143,639	353,398	10,779
1-SI-35-3RR-294Z	144,601	331,148	10,461
1-SI-35-3RR-310N	145,069	143,595	7,507
1-SI-35-3RR-310F	132,993	316,630	9,813
1-SI-35-3RR-314N	132,994	595,022	14,223
1-SI-35-2R-314F	135,495	558,636	13,737
1-SI-35-2R-316N	135,287	442,239	11,885
1-SI-35-2R-316F	135,605	354,324	10,504
1-SI-35-2R-318N	135,493	268,494	9,140
1-SI-35-2R-318F	134,824	206,128	8,128
1-SI-35-2R-320N	133,895	596,295	14,275
1-SI-35-1-320F	132,895	605,939	14,392
1-SI-35-1-326N	140,594	37,566	5,666
1-SI-35-1-330F	144,765	29,682	5,692
1-SI-35-1-334	144,242	18,672	5,499
1-SI-34-1-340	42,031	27,037	1,944
1-SI-34-1-343	40,948	38,853	2,092
1-SI-34-1-344	40,949	50,665	2,280

Notes:

- See Figure 3-5
- Axial force includes pressure

Weld Location Node	Axial Force (lbs)	Moment (in-lbs)	Total Stress (psi)
2-SI-56-10-416	149,651	543,376	14,005
2-SI-56-10-412	150,029	460,335	12,704
2-SI-56-9-406	143,099	371,247	11,042
2-SI-56-9-404Y	143,099	364,094	10,929
2-SI-56-9-404Z	144,000	333,400	10,475
2-SI-56-9-420N	144,458	137,677	7,392
2-SI-56-8-420F	133,182	294,094	9,463
2-SI-56-8-426N	133,182	585,298	14,076
2-SI-56-8-426F	136,019	544,178	13,526
2-SI-56-7-428N	135,811	430,650	11,721
2-SI-56-7-428F	136,040	344,620	10,366
2-SI-56-7-430N	135,930	267,996	9,148
2-SI-56-7-430F	135,377	200,323	8,056
2-SI-56-6-434N	134,428	585,021	14,116
2-SI-56-6-434F	133,012	601,203	14,321
2-SI-56-5-442N	140,759	19,495	5,386
2-SI-56-4-446F	144,982	24,925	5,624
2-SI-56-4-450	144,461	36,168	5,784
2-SI-56-3-456	41,893	46,418	2,246
2-SI-56-3-458F	40,084	70,391	2,561
2-SI-56-3-460	40,083	84,642	2,787

Notes:

- See Figure 3-6
- Axial force includes pressure

Table 3-8 Summary of D.C. Cook Unit 2 Normal Loads and Stresses for 10-inch Accumulator Injection Line Loop 2			
Weld Location Node	Axial Force (lbs)	Moment (in-lbs)	Total Stress (psi)
2-SI-57-10-361	150,058	545,366	14,052
2-SI-57-10-358	150,601	455,303	12,645
2-SI-57-9-352	143,667	352,318	10,763
2-SI-57-9-350X	143,667	342,929	10,614
2-SI-57-9-350Z	137,932	330,093	10,204
2-SI-57-9-348F	137,369	146,848	7,281
2-SI-57-8-348N	148,713	307,489	10,235
2-SI-57-8-344F	148,713	583,312	14,604
2-SI-57-8-344N	145,886	543,484	13,871
2-SI-57-7-342F	146,134	429,243	12,071
2-SI-57-7-342N	146,088	340,780	10,668
2-SI-57-7-340F	146,250	226,938	8,870
2-SI-57-7-340N	146,749	172,793	8,030
2-SI-57-6-338F	147,823	608,808	14,976
2-SI-57-6-338N	148,892	618,226	15,164
2-SI-57-5-332F	141,297	88,253	6,495
2-SI-57-4-332N	141,478	86,492	6,473
2-SI-57-4-326F	141,478	99,948	6,686
2-SI-57-4-326N	142,887	111,859	6,926
2-SI-57-4-324Y	136,719	132,788	7,035
2-SI-57-4-365	136,328	103,172	6,552
2-SI-57-3-368	34,048	115,867	3,064
2-SI-57-3-374	40,010	86,160	2,808

Notes:

- See Figure 3-7
- Axial force includes pressure

Table 3-9 Summary of D.C. Cook Unit 2 Normal Loads and Stresses for 10-inch Accumulator Injection Line Loop 3			
Weld Location Node	Axial Force (lbs)	Moment (in-lbs)	Total Stress (psi)
2-SI-58-10-171	149,588	542,679	13,992
2-SI-58-10-168	150,011	454,313	12,608
2-SI-58-9-162	143,081	351,593	10,731
2-SI-58-9-160Y	143,081	341,851	10,576
2-SI-58-9-160Z	144,042	320,594	10,274
2-SI-58-9-174N	144,604	160,824	7,764
2-SI-58-8-174F	132,871	330,395	10,026
2-SI-58-8-178N	132,871	587,453	14,098
2-SI-58-8-178F	135,786	545,092	13,533
2-SI-58-7-180N	135,537	427,002	11,653
2-SI-58-7-180F	135,723	337,416	10,241
2-SI-58-7-182N	135,592	249,711	8,846
2-SI-58-7-182F	134,989	187,744	7,843
2-SI-58-6-184N	133,878	630,745	14,821
2-SI-58-6-184F	132,765	641,494	14,951
2-SI-58-5-190N	139,574	38,643	5,647
2-SI-58-4-194F	144,633	39,516	5,843
2-SI-58-4-196Y	143,610	43,662	5,872
2-SI-58-4-200	143,270	58,945	6,102
2-SI-58-3-206	40,939	84,090	2,809
2-SI-58-3-212F	38,842	108,533	3,120
2-SI-58-3-214	38,842	106,898	3,094

Notes:

- See Figure 3-8
- Axial force includes pressure

Table 3-10 Summary of D.C. Cook Unit 2 Normal Loads and Stresses for 10-inch Accumulator Injection Line Loop 4			
Weld Location Node	Axial Force (lbs)	Moment (in-lbs)	Total Stress (psi)
2-SI-59-10-307	150,095	554,493	14,198
2-SI-59-10-304	150,649	462,270	12,757
2-SI-59-9-296	143,709	357,048	10,840
2-SI-59-9-294Y	143,715	348,610	10,706
2-SI-59-9-294Z	144,752	338,702	10,587
2-SI-59-9-310N	145,176	138,638	7,433
2-SI-59-8-310F	132,973	312,445	9,746
2-SI-59-8-314N	132,974	596,893	14,252
2-SI-59-8-314F	135,386	561,931	13,785
2-SI-59-7-316N	135,177	445,283	11,930
2-SI-59-7-316F	135,523	357,096	10,545
2-SI-59-7-318N	135,407	271,143	9,179
2-SI-59-7-318F	134,713	208,346	8,160
2-SI-59-6-320N	133,784	597,562	14,292
2-SI-59-6-320F	132,870	605,979	14,392
2-SI-59-5-326N	140,587	40,839	5,718
2-SI-59-4-330F	145,954	33,498	5,795
2-SI-59-4-334	145,430	25,819	5,655
2-SI-59-3-340	42,862	14,809	1,781
2-SI-59-3-344	40,932	35,700	2,042

Notes:

- See Figure 3-9
- Axial force includes pressure

Table 3-11 Summary of D.C. Cook Unit 1 Faulted Loads and Stresses for 10-inch Accumulator Injection Line Loop 1			
Weld Location Node	Axial Force (lbs)	Moment (in-lbs)	Total Stress (psi)
1-SI-29-4-416	153,672	942,766	20,477
1-SI-29-4-412	153,946	781,220	17,928
1-SI-29-3R-406	146,721	541,792	13,875
1-SI-29-3R-404Y	146,708	511,106	13,388
1-SI-29-3R-404Z	148,186	469,759	12,786
1-SI-29-3R-420N	147,785	211,852	8,687
1-SI-29-3R-420F	150,017	359,241	11,102
1-SI-29-2-426N	149,655	665,307	15,937
1-SI-29-2-426F	147,300	650,728	15,621
1-SI-29-2-428N	147,466	585,585	14,595
1-SI-29-2-428F	148,333	485,703	13,044
1-SI-29-2-430N	148,854	253,259	9,381
1-SI-29-2-430F	148,404	265,934	9,566
1-SI-29-2-434N	149,155	664,249	15,902
1-SI-29-1-434F	150,250	654,108	15,781
1-SI-29-1-442N	143,611	203,227	8,399
1-SI-29-1-446F	149,385	157,310	7,880
1-SI-29-1-450	148,910	210,917	8,712
1-SI-28-1-456	46,553	312,358	6,627
1-SI-28-1-459	43,989	325,555	6,744

Notes:

- See Figure 3-2
- Axial force includes pressure

Weld Location Node	Axial Force (lbs)	Moment (in-lbs)	Total Stress (psi)
1-SI-31-4-361	154,404	952,033	20,650
1-SI-31-4-358	152,740	789,100	18,009
1-SI-31-3R-352	145,511	548,357	13,935
1-SI-31-3R-350X	145,498	508,389	13,301
1-SI-31-3R-350Z	147,631	486,646	13,034
1-SI-31-3R-348F	147,051	240,974	9,121
1-SI-31-3R-348N	149,869	372,305	11,303
1-SI-31-3R-344F	149,387	638,071	15,496
1-SI-31-2-344N	147,035	610,125	14,968
1-SI-31-2-342F	147,236	495,600	13,162
1-SI-31-2-342N	146,912	408,000	11,762
1-SI-31-2-340F	147,103	288,840	9,882
1-SI-31-2-340N	147,764	231,000	8,989
1-SI-31-1A-338F	148,728	689,316	16,284
1-SI-31-1A-338N	149,712	673,084	16,062
1-SI-31-1A-332F	146,225	140,085	7,493
1-SI-31-1A-332N	147,023	154,999	7,758
1-SI-31-1A-330F	146,976	128,480	7,337
1-SI-31-1A-324	141,935	139,947	7,337
1-SI-31-1A-324Y	145,662	297,275	9,963
1-SI-31-1A-365	145,212	171,169	7,949
1-SI-30-1-369N	42,645	121,272	3,459
1-SI-30-1-372F	45,895	141,382	3,895
1-SI-30-1-374	45,911	133,357	3,768

Notes:

- See Figure 3-3
- Axial force includes pressure

Table 3-13 Summary of D.C. Cook Unit 1 Faulted Loads and Stresses for 10-inch Accumulator Injection Line Loop 3			
Weld Location Node	Axial Force (lbs)	Moment (in-lbs)	Total Stress (psi)
1-SI-33-4-171	154,449	901,426	19,850
1-SI-33-4-168	151,850	761,463	17,539
1-SI-33-3R-162	144,623	536,440	13,714
1-SI-33-3R-160Y	144,616	498,873	13,119
1-SI-33-3R-160Z	147,423	442,778	12,332
1-SI-33-3R-174N	146,959	258,020	9,388
1-SI-33-3R-174F	149,946	400,054	11,746
1-SI-33-3R-178N	149,575	640,568	15,542
1-SI-33-2-178F	147,267	609,999	14,975
1-SI-33-2-180N	147,477	485,807	13,015
1-SI-33-2-180F	146,974	397,219	11,594
1-SI-33-2-182N	147,107	301,798	10,087
1-SI-33-2-182F	147,947	237,093	9,092
1-SI-33-2-184N	148,927	694,425	16,372
1-SI-33-1A-184F	149,821	711,587	16,676
1-SI-33-1A-190N	144,313	276,976	9,593
1-SI-33-1A-196	143,545	304,639	10,003
1-SI-33-1A-196Y	149,256	399,444	11,711
1-SI-33-1A-200	148,879	255,528	9,418
1-SI-32-1-206	46,374	222,432	5,196
1-SI-32-1-214	48,770	239,236	5,549

Notes:

- See Figure 3-4
- Axial force includes pressure

Table 3-14 Summary of D.C. Cook Unit 1 Faulted Loads and Stresses for 10-inch Accumulator Injection Line Loop 4			
Weld Location Node	Axial Force (lbs)	Moment (in-lbs)	Total Stress (psi)
1-SI-35-4-307	154,554	933,994	20,370
1-SI-35-4-304	152,576	766,603	17,647
1-SI-35-3RR-296	145,345	521,590	13,505
1-SI-35-3RR-294Y	145,332	485,618	12,935
1-SI-35-3RR-294Z	147,986	474,798	12,859
1-SI-35-3RR-310N	147,518	218,605	8,784
1-SI-35-3RR-310F	149,705	368,180	11,232
1-SI-35-3RR-314N	149,405	635,330	15,453
1-SI-35-2R-314F	147,354	613,318	15,031
1-SI-35-2R-316N	147,555	500,811	13,256
1-SI-35-2R-316F	146,931	417,057	11,906
1-SI-35-2R-318N	147,080	330,240	10,536
1-SI-35-2R-318F	148,019	263,726	9,517
1-SI-35-2R-320N	149,016	669,413	15,979
1-SI-35-1-320F	149,633	653,715	15,753
1-SI-35-1-326N	142,784	201,489	8,342
1-SI-35-1-330F	147,894	156,026	7,806
1-SI-35-1-334	147,326	155,105	7,771
1-SI-34-1-340	45,110	231,951	5,301
1-SI-34-1-343	43,528	244,127	5,437
1-SI-34-1-344	43,360	222,408	5,087

Notes:

- See Figure 3-5
- Axial force includes pressure

Table 3-15 Summary of D.C. Cook Unit 2 Faulted Loads and Stresses for 10-inch Accumulator Injection Line Loop 1			
Weld Location Node	Axial Force (lbs)	Moment (in-lbs)	Total Stress (psi)
2-SI-56-10-416	154,850	881,028	19,542
2-SI-56-10-412	152,074	738,135	17,178
2-SI-56-9-406	144,653	540,790	13,784
2-SI-56-9-404Y	144,644	510,587	13,305
2-SI-56-9-404Z	147,675	474,565	12,844
2-SI-56-9-420N	147,200	221,137	8,813
2-SI-56-8-420F	149,883	360,838	11,122
2-SI-56-8-426N	149,401	635,776	15,460
2-SI-56-8-426F	146,934	605,903	14,898
2-SI-56-7-428N	147,130	496,465	13,171
2-SI-56-7-428F	146,624	409,344	11,773
2-SI-56-7-430N	146,754	330,436	10,528
2-SI-56-7-430F	147,567	261,721	9,469
2-SI-56-6-434N	148,583	654,713	15,731
2-SI-56-6-434F	149,711	649,740	15,693
2-SI-56-5-442N	143,803	225,713	8,763
2-SI-56-4-446F	149,901	169,423	8,091
2-SI-56-4-450	149,341	224,348	8,941
2-SI-56-3-456	46,670	334,073	6,975
2-SI-56-3-458F	44,438	339,098	6,974
2-SI-56-3-460	44,252	297,910	6,315

Notes:

- See Figure 3-6
- Axial force includes pressure

Table 3-16 Summary of D.C. Cook Unit 2 Faulted Loads and Stresses for 10-inch Accumulator Injection Line Loop 2			
Weld Location Node	Axial Force (lbs)	Moment (in-lbs)	Total Stress (psi)
2-SI-57-10-361	154,785	930,327	20,320
2-SI-57-10-358	152,910	780,228	17,875
2-SI-57-9-352	145,580	550,743	13,975
2-SI-57-9-350X	145,569	511,768	13,358
2-SI-57-9-350Z	147,817	481,026	12,952
2-SI-57-9-348F	147,242	247,668	9,234
2-SI-57-8-348N	150,193	383,617	11,494
2-SI-57-8-344F	149,631	639,502	15,527
2-SI-57-8-344N	147,232	612,808	15,018
2-SI-57-7-342F	147,461	500,072	13,241
2-SI-57-7-342N	147,082	408,334	11,774
2-SI-57-7-340F	147,290	289,277	9,895
2-SI-57-7-340N	148,059	237,803	9,108
2-SI-57-6-338F	149,189	689,628	16,306
2-SI-57-6-338N	149,941	674,341	16,091
2-SI-57-5-332F	144,134	265,896	9,411
2-SI-57-4-332N	144,113	261,199	9,336
2-SI-57-4-326F	144,098	251,473	9,181
2-SI-57-4-326N	143,623	256,107	9,237
2-SI-57-4-324Y	147,576	407,080	11,772
2-SI-57-4-365	147,983	281,549	9,798
2-SI-57-3-368	49,754	210,309	5,126
2-SI-57-3-374	43,079	187,522	4,524

Notes:

- See Figure 3-7
- Axial force includes pressure

Table 3-17 Summary of D.C. Cook Unit 2 Faulted Loads and Stresses for 10-inch Accumulator Injection Line Loop 3			
Weld Location Node	Axial Force (lbs)	Moment (in-lbs)	Total Stress (psi)
2-SI-58-10-171	155,131	963,864	20,864
2-SI-58-10-168	152,408	816,935	18,438
2-SI-58-9-162	145,111	586,733	14,529
2-SI-58-9-160Y	145,101	546,305	13,888
2-SI-58-9-160Z	147,868	482,583	12,978
2-SI-58-9-174N	147,313	276,331	9,691
2-SI-58-8-174F	150,295	414,861	11,993
2-SI-58-8-178N	149,785	648,744	15,679
2-SI-58-8-178F	147,541	620,256	15,147
2-SI-58-7-180N	147,779	497,191	13,206
2-SI-58-7-180F	147,170	409,449	11,794
2-SI-58-7-182N	147,331	312,371	10,262
2-SI-58-7-182F	148,328	248,448	9,286
2-SI-58-6-184N	149,512	720,276	16,803
2-SI-58-6-184F	150,085	729,325	16,967
2-SI-58-5-190N	144,043	183,813	8,107
2-SI-58-4-194F	156,146	220,688	9,128
2-SI-58-4-196Y	147,601	338,570	10,687
2-SI-58-4-200	147,198	202,172	8,512
2-SI-58-3-206	44,594	160,676	4,154
2-SI-58-3-212F	47,965	208,334	5,030
2-SI-58-3-214	47,974	196,809	4,848

Notes:

- See Figure 3-8
- Axial force includes pressure

Table 3-18 Summary of D.C. Cook Unit 2 Faulted Loads and Stresses for 10-inch Accumulator Injection Line Loop 4			
Weld Location Node	Axial Force (lbs)	Moment (in-lbs)	Total Stress (psi)
2-SI-59-10-307	155,202	970,257	20,968
2-SI-59-10-304	152,894	794,224	18,096
2-SI-59-9-296	145,478	534,370	13,712
2-SI-59-9-294Y	145,476	494,266	13,077
2-SI-59-9-294Z	147,968	483,080	12,990
2-SI-59-9-310N	147,567	228,424	8,941
2-SI-59-8-310F	149,838	371,593	11,291
2-SI-59-8-314N	149,475	641,406	15,552
2-SI-59-8-314F	147,647	624,363	15,216
2-SI-59-7-316N	147,848	509,412	13,402
2-SI-59-7-316F	147,148	421,203	11,980
2-SI-59-7-318N	147,299	331,829	10,570
2-SI-59-7-318F	148,309	267,901	9,593
2-SI-59-6-320N	149,290	674,205	16,065
2-SI-59-6-320F	149,797	656,912	15,809
2-SI-59-5-326N	143,537	236,480	8,923
2-SI-59-4-330F	149,661	188,469	8,384
2-SI-59-4-334	149,098	190,010	8,388
2-SI-59-3-340	46,391	276,428	6,052
2-SI-59-3-344	44,025	292,096	6,215

Notes:

- See Figure 3-9
- Axial force includes pressure

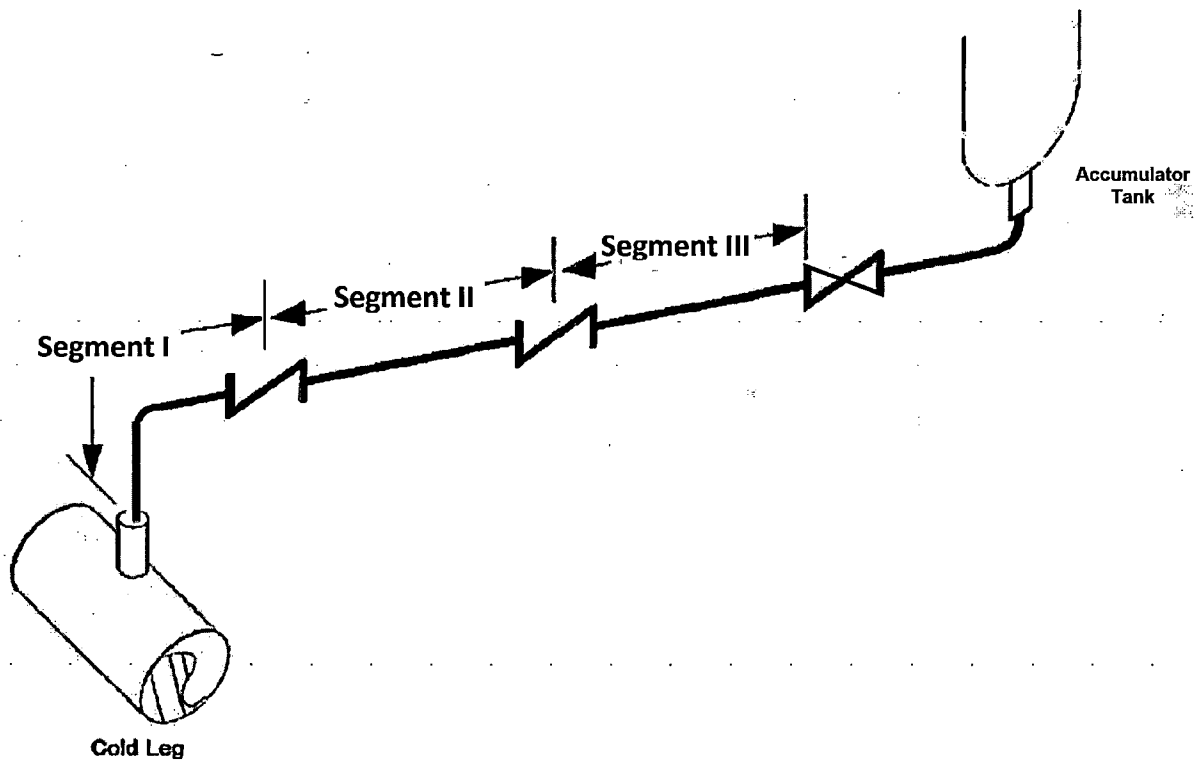


Figure 3-1 10-inch Accumulator Line Layout Showing Segments for D.C. Cook Units 1 and 2

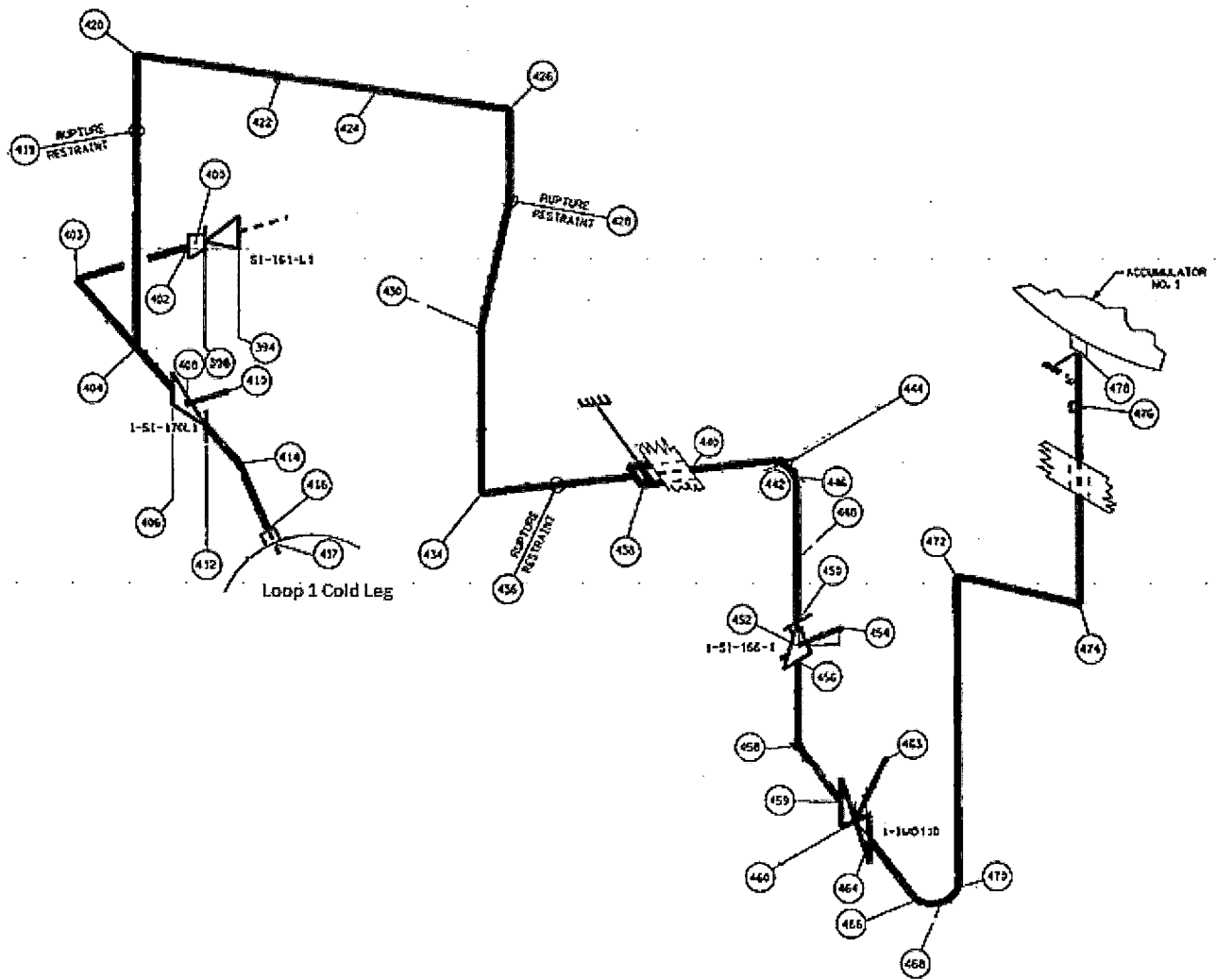


Figure 3-2 D.C. Cook Unit 1 Accumulator Line Loop 1 Layout Showing Weld Locations with Node Points

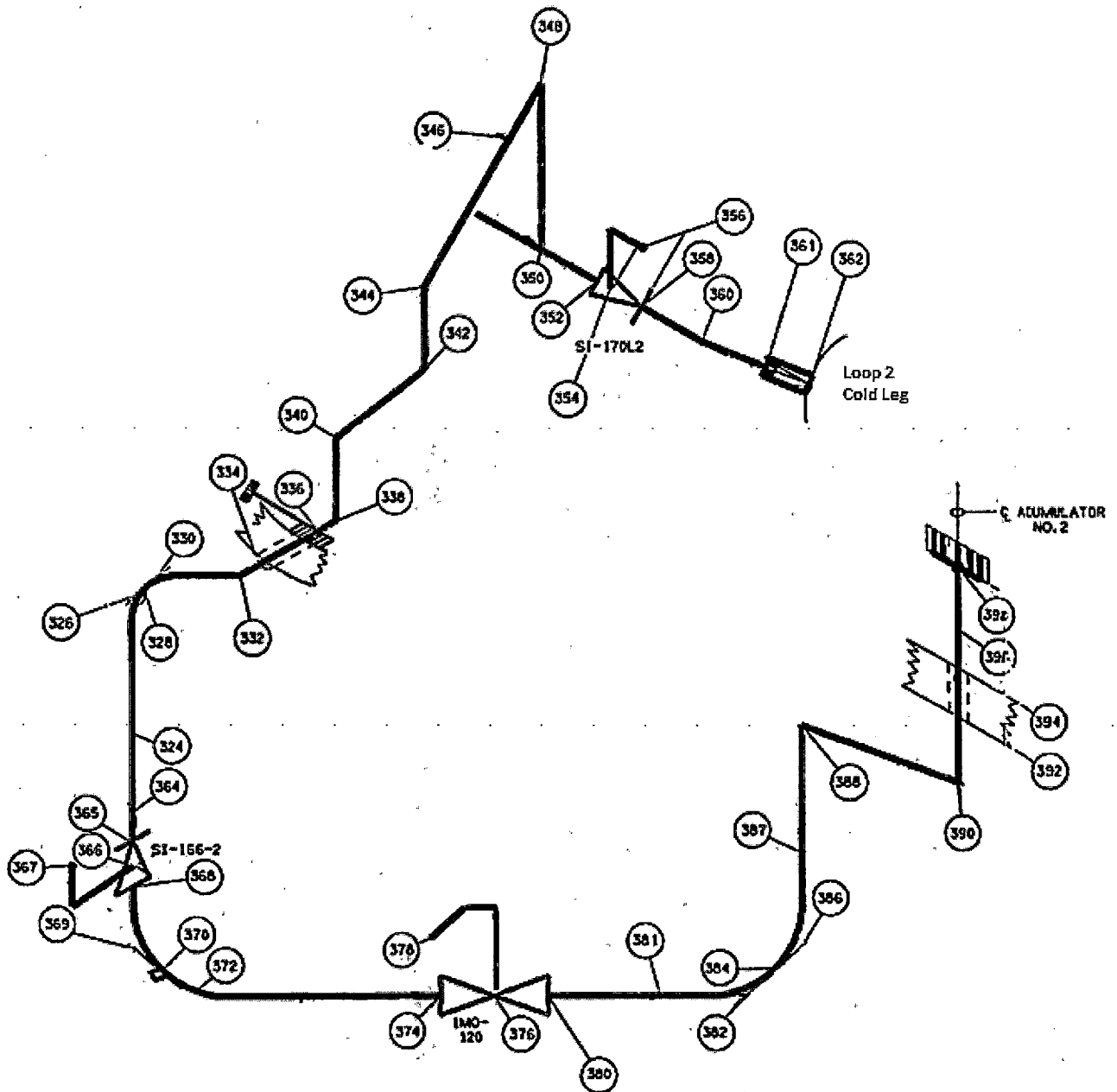


Figure 3-3 D.C. Cook Unit 1 Accumulator Line Loop 2 Layout Showing Weld Locations with Node Points

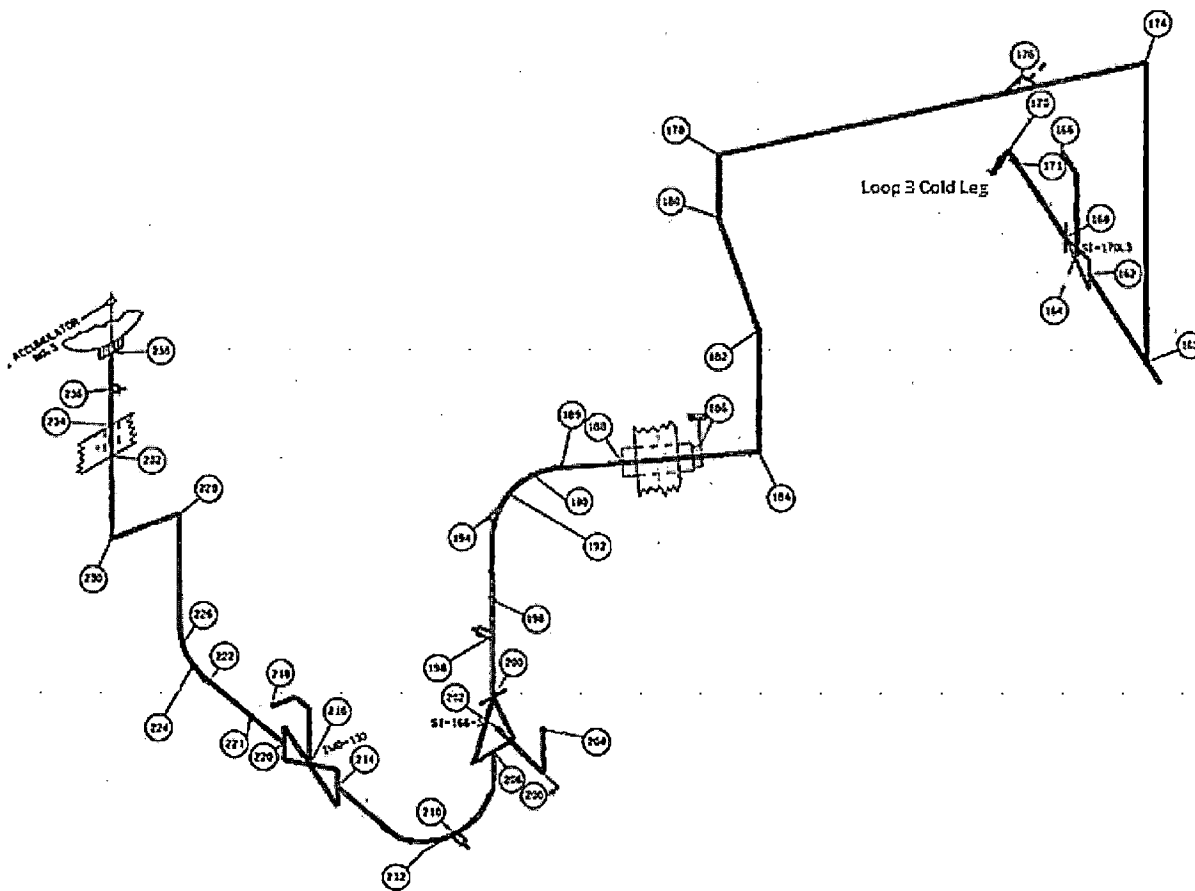


Figure 3-4 D.C. Cook Unit 1 Accumulator Line Loop 3 Layout Showing Weld Locations with Node Points

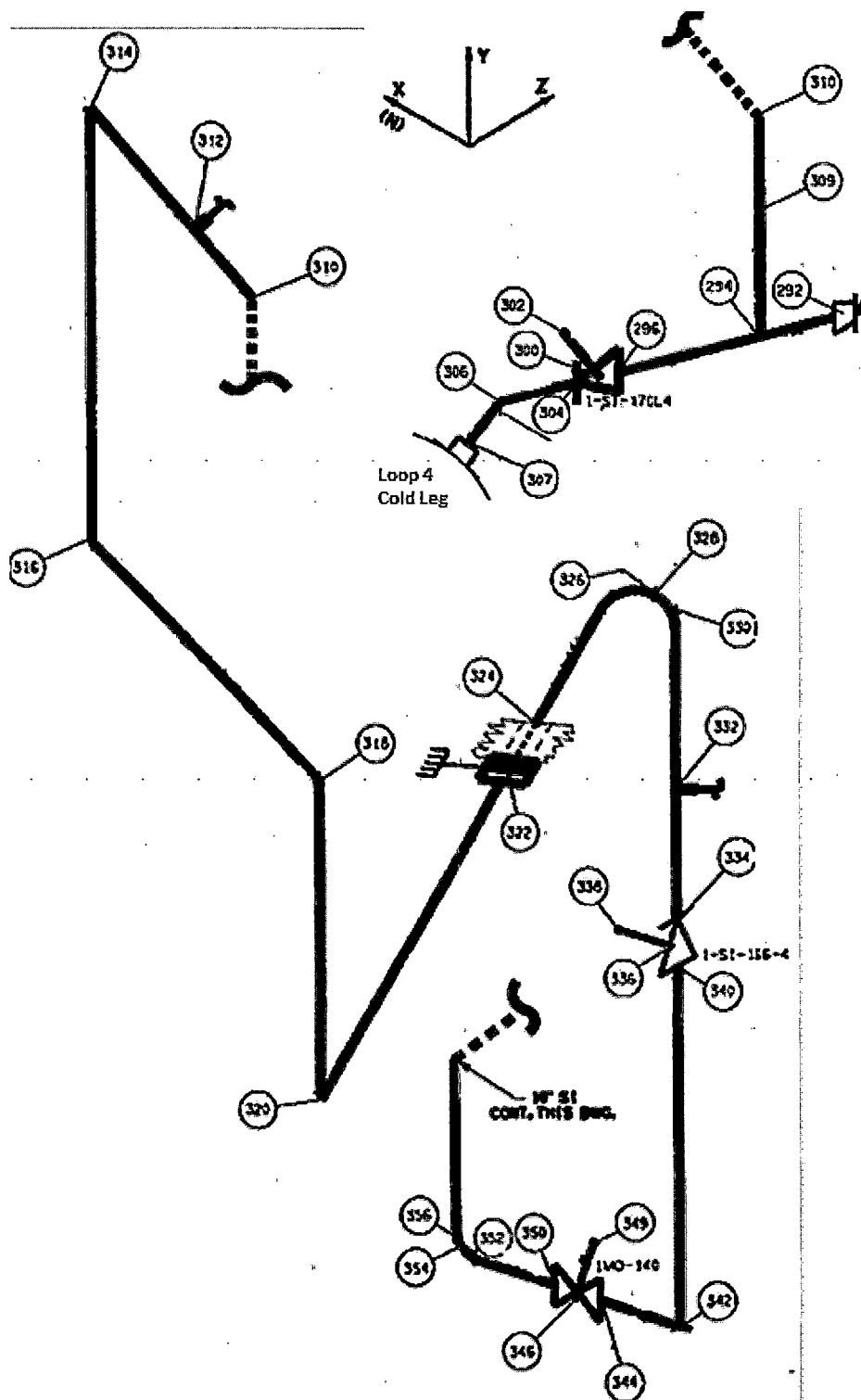


Figure 3-5 D.C. Cook Unit 1 Accumulator Line Loop 4 Layout Showing Weld Locations with Node Points

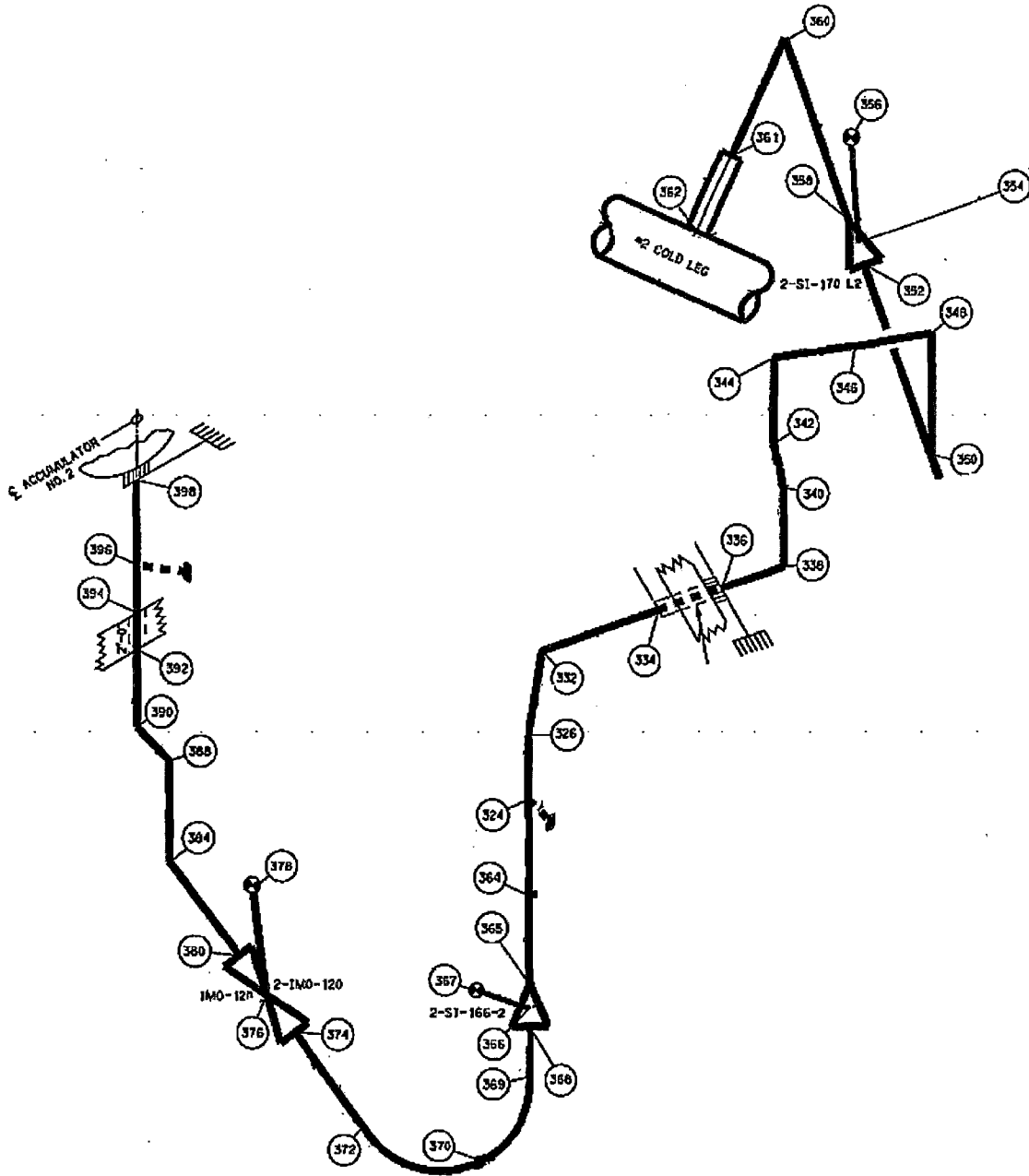


Figure 3-7 D.C. Cook Unit 2 Accumulator Line Loop 2 Layout Showing Weld Locations with Node Points

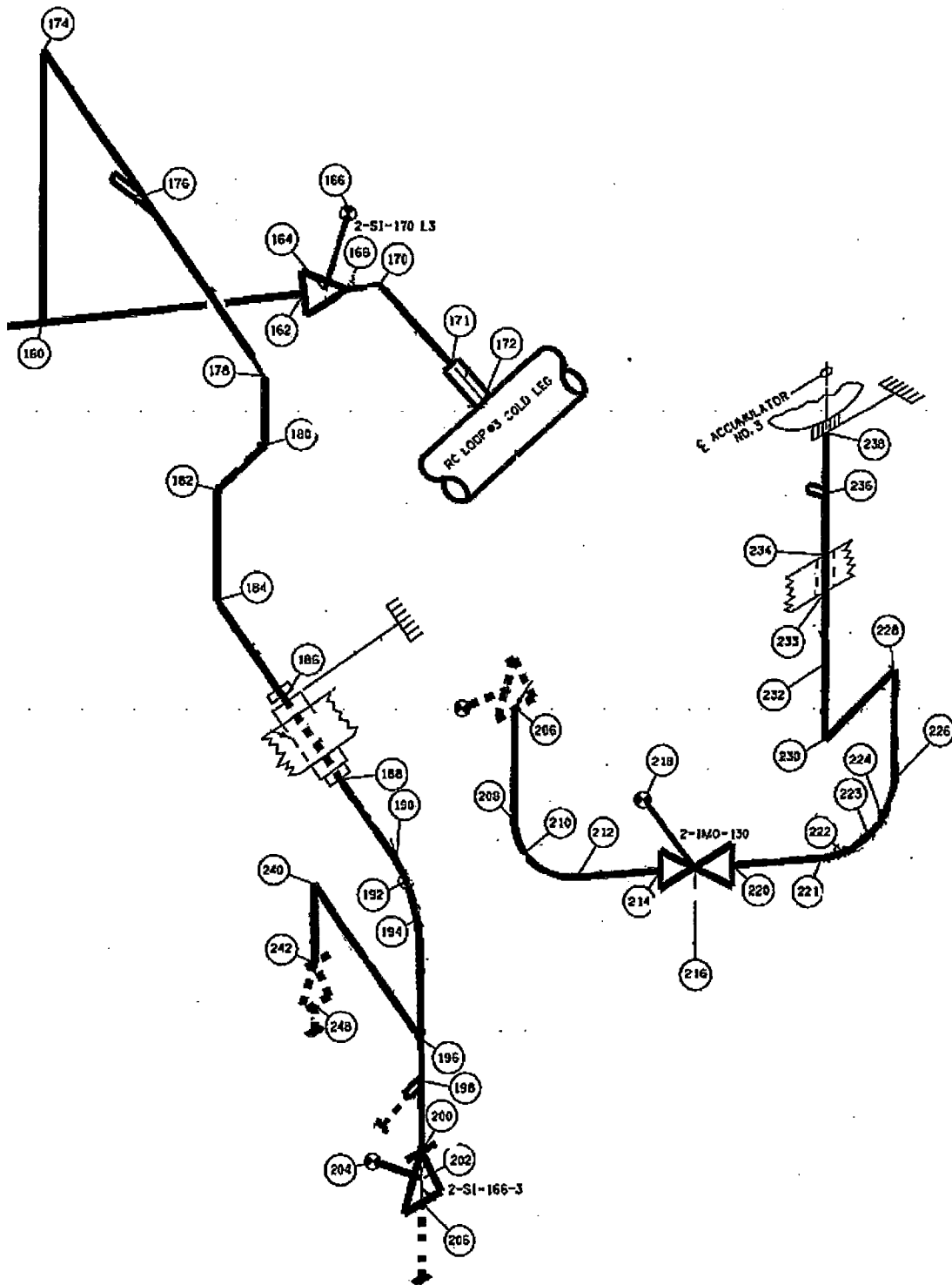
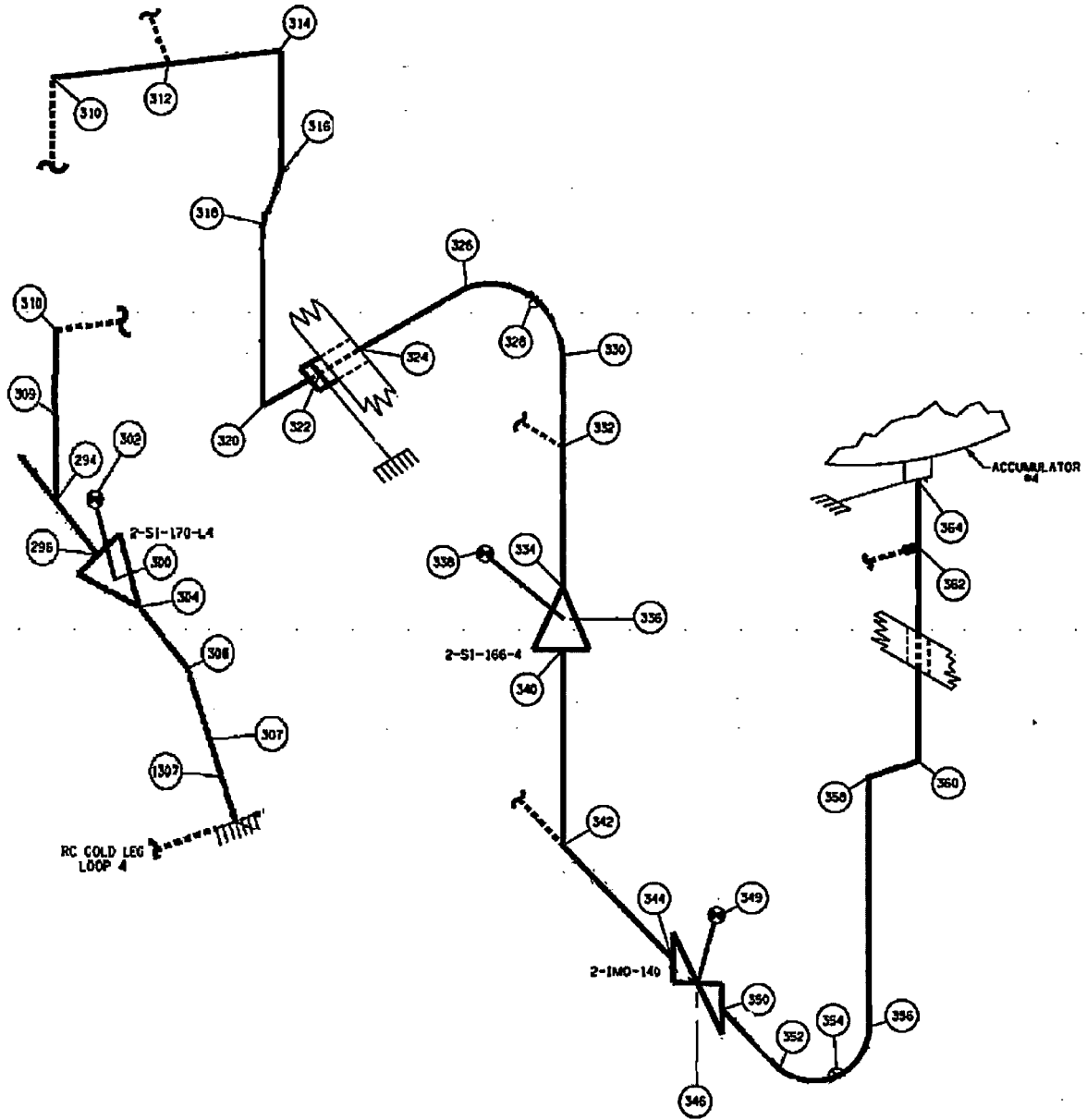


Figure 3-8 D.C. Cook Unit 2 Accumulator Line Loop 3 Layout Showing Weld Locations with Node Points



4.0 MATERIAL CHARACTERIZATION

4.1 ACCUMULATOR LINE PIPE MATERIAL AND WELD PROCESS

The material type of the accumulator line for D.C. Cook Units 1 and 2 is A376 TP316 (seamless pipe) and A403 WP316 (wrought fittings) for the pipe and fittings, respectively. The welding processes used are Submerged Arc Weld (SAW) and Shielded Metal Arc Weld (SMAW).

In the following sections the tensile properties of the materials are presented for use in the Leak-Before-Break analyses.

4.2 TENSILE PROPERTIES

Certified Material Test Reports (CMTRs) with mechanical properties were not readily available for the D.C. Cook Units 1 and 2 accumulator lines. For the D.C. Cook Units 1 and 2 accumulator lines, the ASME Code mechanical properties were used to establish the tensile properties for the Leak-Before-Break analyses. The tensile properties for the pipe material are provided in Table 4-1 for the Units 1 and 2 accumulator lines.

For the A376 TP316 pipe material and the A403 WP316 fitting material, the representative properties at operating temperatures are established from the tensile properties interpolated from Section II of the ASME Boiler and Pressure Vessel Code (Reference 4-1). Code tensile properties at the operating temperatures were obtained by interpolating between various tensile Code properties.

The modulus of elasticity value was also interpolated from ASME Code properties, and Poisson's ratio was taken as 0.3.

4.3 REFERENCE

- 4-1 ASME Boiler and Pressure Vessel Code, Section II, Part D, "Properties (Customary) Materials," 2007 Edition up to and including 2008 Addenda.

Material	Temperature (°F)	Modulus of Elasticity (E) (ksi)	Yield Strength (psi)	Ultimate Strength (psi)
A376 TP316 A403 WP316	549	25,606	19,461	71,800
A376 TP316 A403 WP316	120	27,992	28,960	75,000

5.0 CRITICAL LOCATIONS

5.1 CRITICAL LOCATIONS

The Leak-Before-Break (LBB) evaluation margins are to be demonstrated for the critical locations (governing locations). Such locations are established based on the loads (Section 3.3) and the material properties established in Section 4.2. These locations are defined below for the D.C. Cook accumulator lines.

Critical Locations for the 10-inch accumulator lines (see Table 5-1):

The welds in the accumulator line are fabricated using Shielded Metal Arc Weld (SMAW) and Submerged Arc Weld (SAW) for field and shop welds. The pipe material type is A376 TP 316 or A403 WP316 which have identical material properties. The governing locations were established on the basis of the pipe geometry, material type, operating temperature, operating pressure, and the highest faulted stresses at the welds.

Table 5-1 shows the highest faulted stresses and the corresponding weld location node for each welding process type in each segment of the 10-inch accumulator lines, enveloping both D.C. Cook Units 1 and 2. Definition of the piping segments and the corresponding operating pressure and temperature parameters are from Tables 3-1 and 3-2. Figures 5-1 through 5-3 show the location of the critical welds.

Segment	Pipe Size	Welding Process	Operating Pressure (psig)	Operating Temperature (°F)	Maximum Faulted Stress (psi)	Weld Location Node
I	10-inch	SMAW	2,345	549	20,968	2-SI-59-10-307
II	10-inch	SAW	2,235	549	13,888	2-SI-58-9-160Y
		SMAW	2,235	549	14,529	2-SI-58-9-162
		SAW	2,235	120	16,803	2-SI-58-6-184N
		SMAW	2,235	120	16,967	2-SI-58-6-184F
III	10-inch	SAW	644	120	6,974	2-SI-56-3-458F
		SMAW	644	120	6,975	2-SI-56-3-456

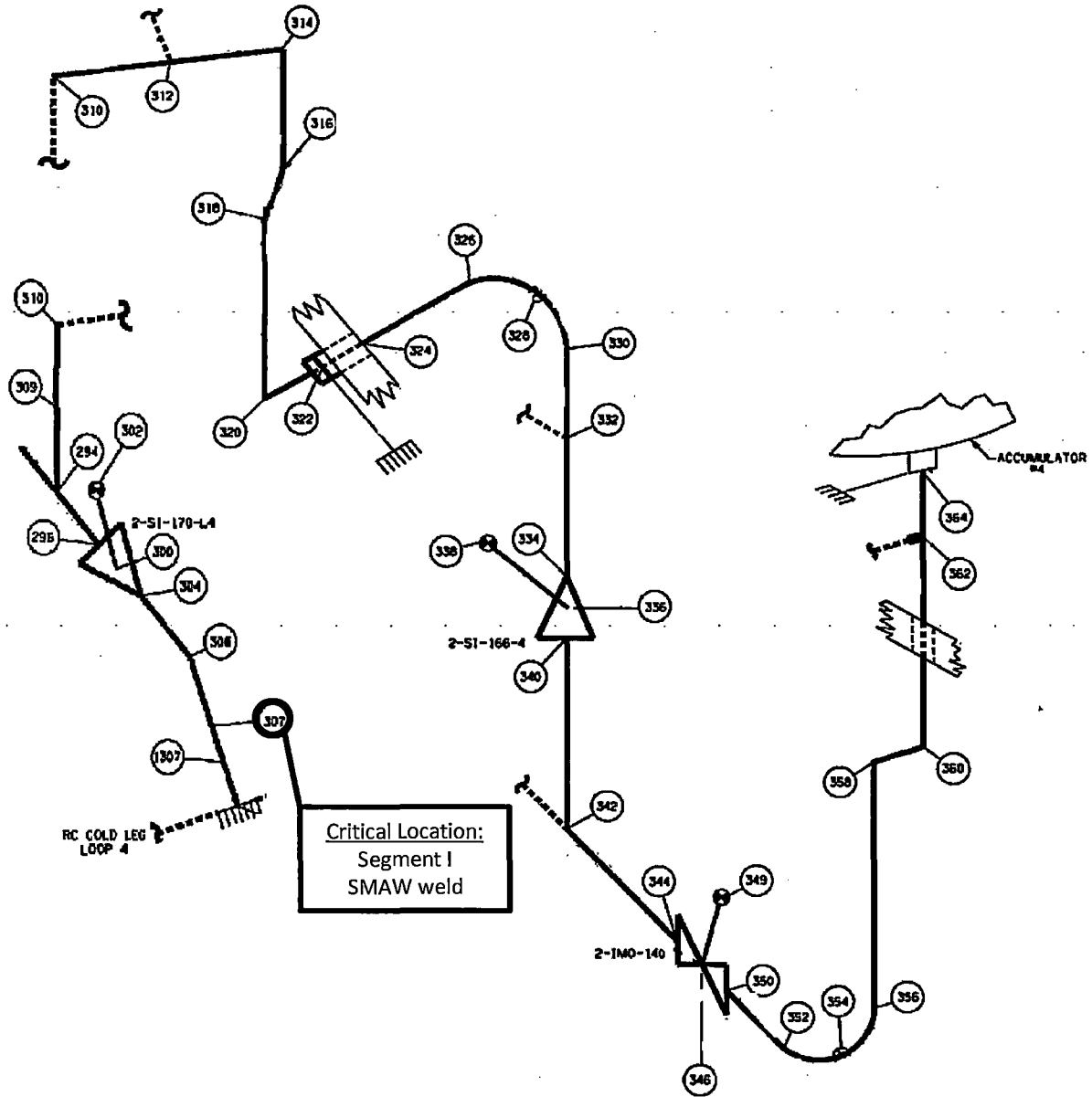


Figure 5-1 Layout Showing Critical Location Loop 4 Unit 2

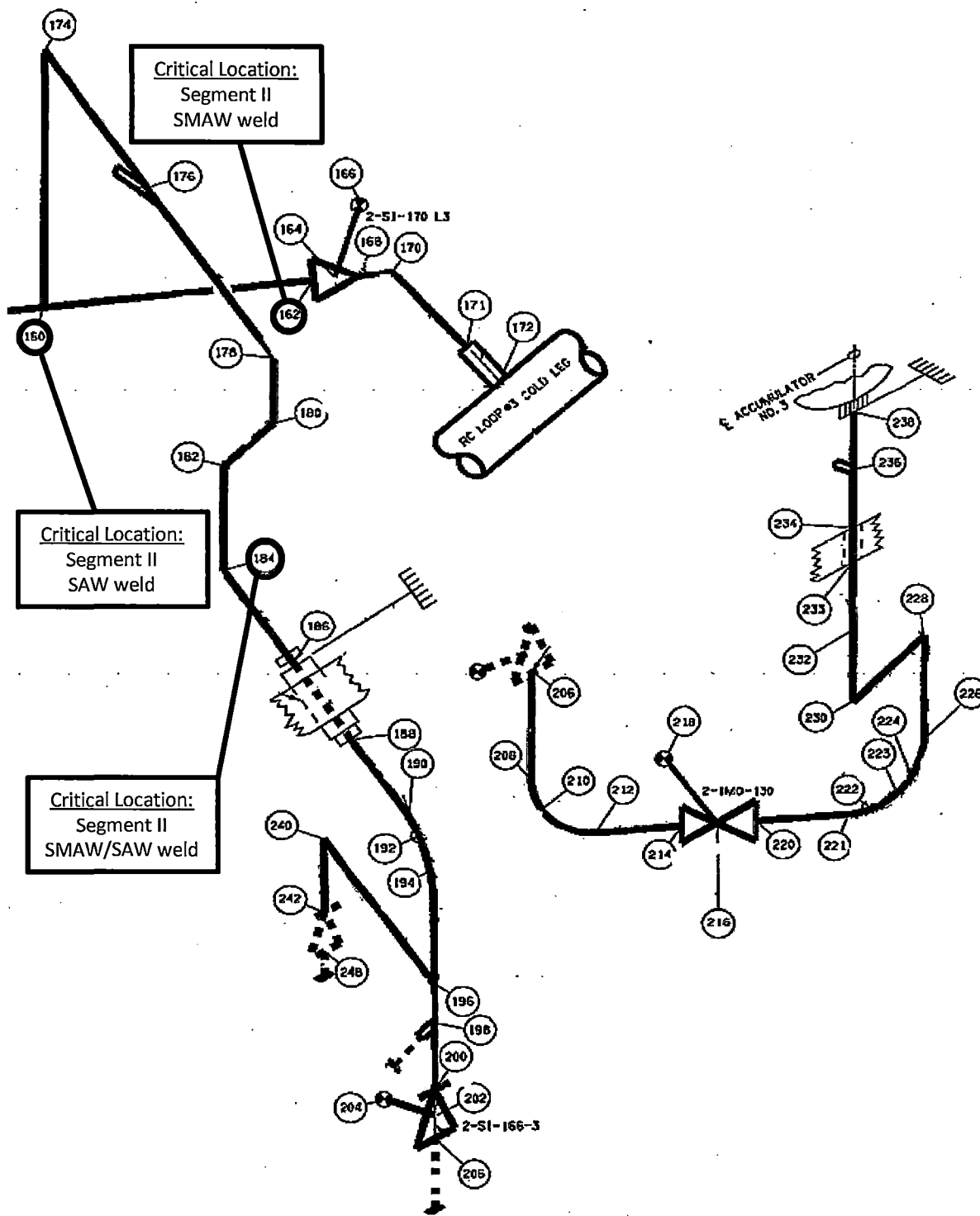


Figure 5-2 Layout Showing Critical Locations Loop 3 Unit 2

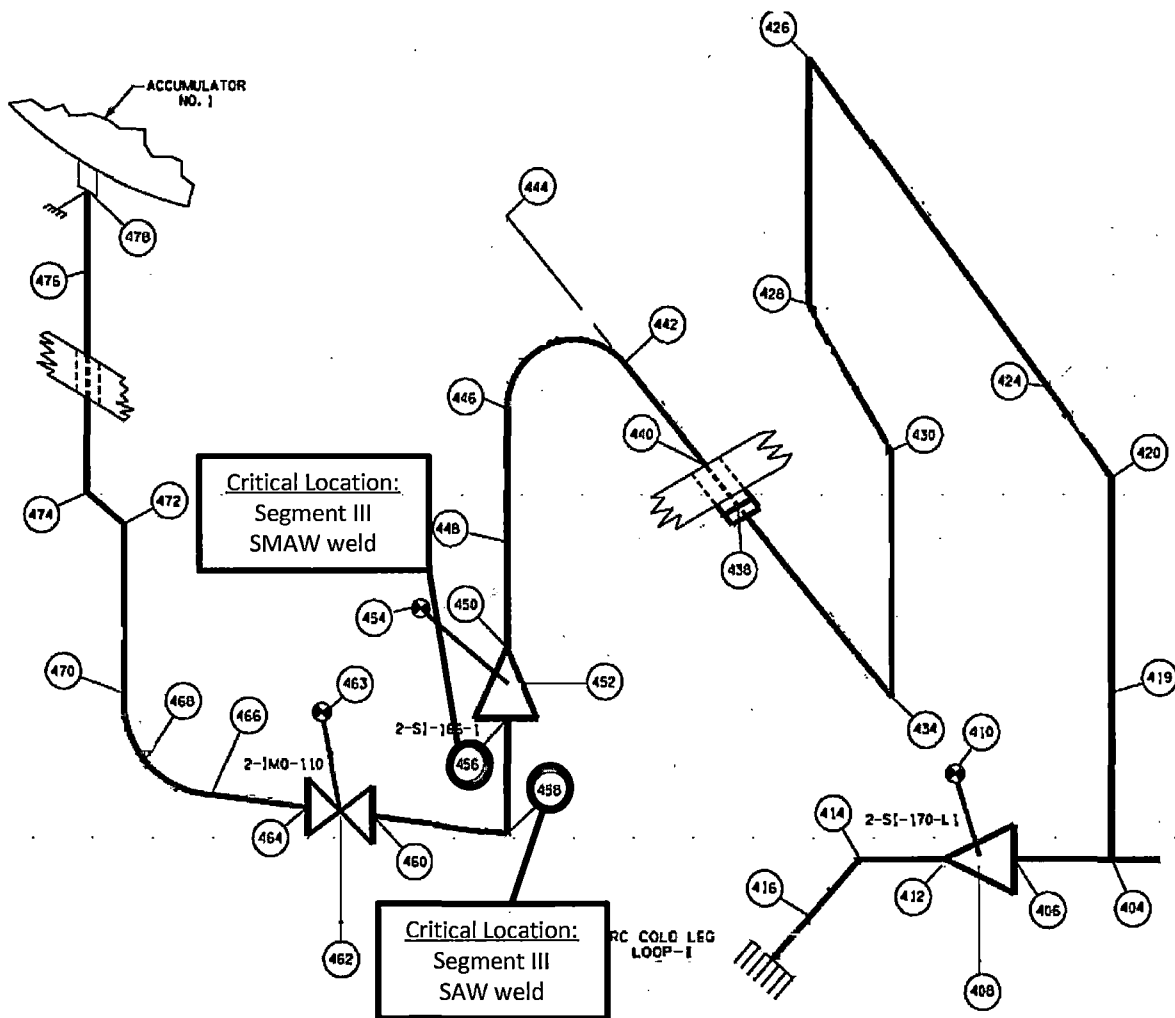


Figure 5-3 Layout Showing Critical Locations Loop 1 Unit 2

6.0 LEAK RATE PREDICTIONS

6.1 INTRODUCTION

The purpose of this section is to discuss the method which is used to predict the flow through postulated through-wall cracks and present the leak rate calculation results for through-wall circumferential cracks.

6.2 GENERAL CONSIDERATIONS

The flow of hot pressurized water through an opening to a lower back pressure causes flashing which can result in choking. For long channels where the ratio of the channel length, L , to hydraulic diameter, D_H , (L/D_H) is greater than [

]^{a,c,e}

6.3 CALCULATION METHOD

The basic method used in the leak rate calculations is the method developed by [

]^{a,c,e}

The flow rate through a crack was calculated in the following manner. Figure 6-1 (from Reference 6-2) was used to estimate the critical pressure, P_c , for the accumulator line enthalpy condition and an assumed flow. Once P_c was found for a given mass flow, the []^{a,c,e} was found from Figure 6-2 (taken from Reference 6-2). For all cases considered, []^{a,c,e} therefore, this method will yield the two-phase pressure drop due to momentum effects as illustrated in Figure 6-3, where P_o is the operating pressure. Now using the assumed flow rate, G , the frictional pressure drop can be calculated using

$$\Delta P_f = []^{\text{a,c,e}} \quad (6-1)$$

where the friction factor f is determined using the []^{a,c,e} The crack relative roughness, ϵ , was obtained from fatigue crack data on stainless steel samples. The relative roughness value used in these calculations was []^{a,c,e}

The frictional pressure drop using equation 6-1 is then calculated for the assumed flow rate and added to the []^{a,c,e} to obtain the total pressure drop from the primary system to the atmosphere.

That is, for the accumulator line:

$$\text{Absolute Pressure} - 14.7 = [\quad \quad \quad]^{a,c,e} \quad (6-2)$$

for a given assumed flow rate G. If the right-hand side of equation 6-2 does not agree with the pressure difference between the accumulator line and the atmosphere, then the procedure is repeated until equation 6-2 is satisfied to within an acceptable tolerance which in turn leads to a flow rate value for a given crack size.

For the single phase cases with lower temperature, leakage rate is calculated by the following equation (Reference 6-4) with the crack opening area obtained by the method from Reference 6-3.

$$Q = A (2g\Delta P/k\rho)^{0.5} \text{ ft}^3/\text{sec}; \quad (6-3)$$

Where, ΔP = pressure difference between stagnation and back pressure (lb/ft²), g = acceleration of gravity (ft/sec²), ρ = fluid density at atmospheric pressure (lb/ft³), k = friction loss including passage loss, inlet and outlet of the through-wall crack, A = crack opening area (ft²).

6.4 LEAK RATE CALCULATIONS

Leak rate calculations were made as a function of crack length at the governing locations previously identified in Section 5.1. The normal operating loads of Table 3-3 through Table 3-6 (for Unit 1), and Table 3-7 through Table 3-10 (for Unit 2) were applied, in these calculations. The crack opening areas were estimated using the method of Reference 6-3 and the leak rates were calculated using the formulation described above. The material properties of Section 4.2 (see Table 4-1) were used for these calculations.

The flaw sizes to yield a leak rate of 8 gpm were calculated at the governing locations and are given in Table 6-1 for D.C. Cook Unit 1 and Unit 2. The flaw sizes so determined are called leakage flaw sizes.

The D.C. Cook Unit 1 and 2 RCS pressure boundary leak detection system meets the intent of Regulatory Guide 1.45 and meets a leak detection capability of 0.8 gpm. Thus, to satisfy the margin of 10 on the leak rate, the flaw sizes (leakage flaw sizes) are determined which yield a leak rate of 8 gpm.

6.5 REFERENCES

- 6-1 []^{a,c,e}
- 6-2 M. M, El-Wakil, "Nuclear Heat Transport, International Textbook Company," New York, N.Y, 1971.
- 6-3 Tada, H., "The Effects of Shell Corrections on Stress Intensity Factors and the Crack Opening Area of Circumferential and a Longitudinal Through-Crack in a Pipe," Section II-1, NUREG/CR-3464, September 1983.
- 6-4 Crane, D. P., "Handbook of Hydraulic Resistance Coefficient," Flow of Fluids through Valves, Fittings, and Pipe by the Engineering Division of Crane, 1981, Technical Paper No. 410.

Segment	Pipe Size	Welding Process	Weld Location Node	Leakage Flow Size (in)
I	10-inch	SMAW	2-SI-59-10-307	2.79
II	10-inch	SAW	2-SI-58-9-160Y	3.68
		SMAW	2-SI-58-9-162	3.64
		SAW	2-SI-58-6-184N	3.03
		SMAW	2-SI-58-6-184F	3.01
III	10-inch	SAW	2-SI-56-3-458F	9.17
		SMAW	2-SI-56-3-456	9.57

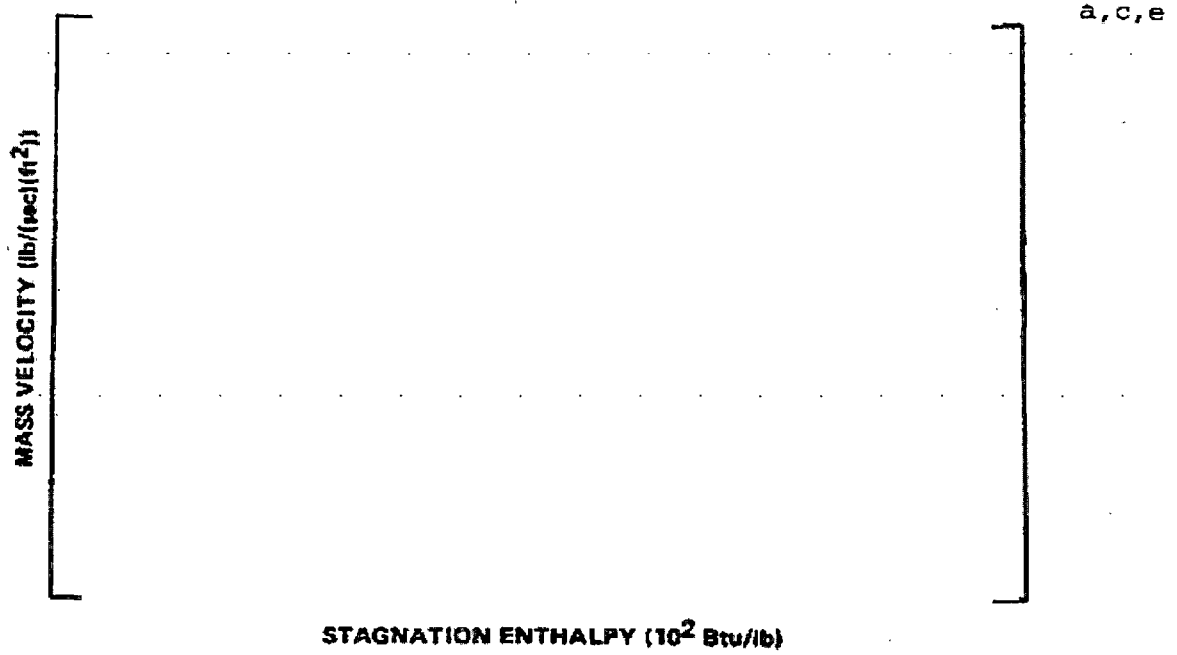


Figure 6-1 Analytical Predictions of Critical Flow Rates of Steam-Water Mixtures

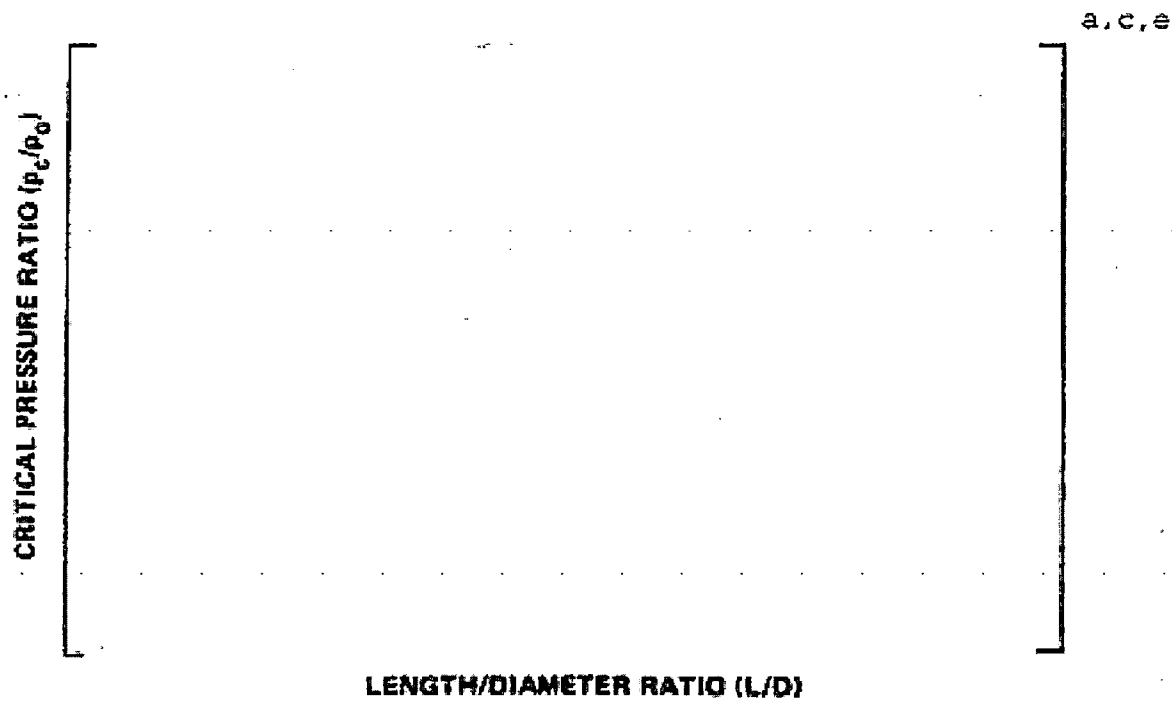


Figure 6-2 []^{a,c,e} Pressure Ratio as a Function of L/D

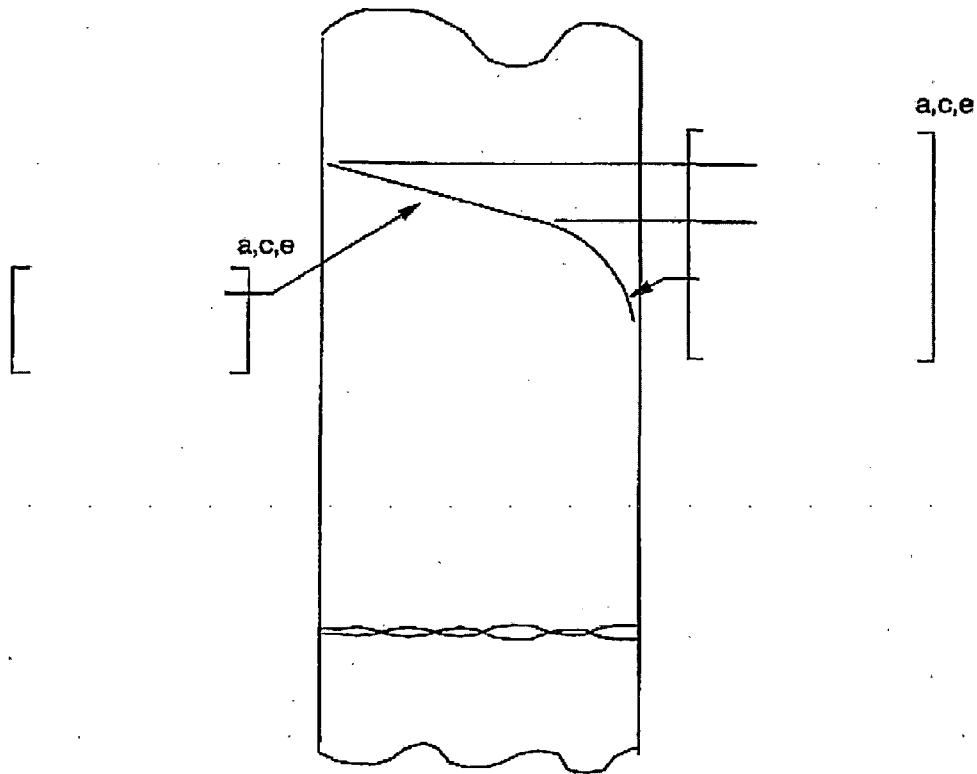


Figure 6-3 Idealized Pressure Drop Profile Through a Postulated Crack

7.0 FRACTURE MECHANICS EVALUATION

7.1 GLOBAL FAILURE MECHANISM

Determination of the conditions which lead to failure in stainless steel should be done with plastic fracture methodology because of the large amount of deformation accompanying fracture. One method for predicting the failure of ductile material is the plastic instability method, based on traditional plastic limit load concepts, but accounting for strain hardening and taking into account the presence of a flaw. The flawed pipe is predicted to fail when the remaining net section reaches a stress level at which a plastic hinge is formed. The stress level at which this occurs is termed as the flow stress. The flow stress is generally taken as the average of the yield and ultimate tensile strength of the material at the temperature of interest. This methodology has been shown to be applicable to ductile piping through a large number of experiments and will be used here to predict the critical flaw size in accumulator line piping. The failure criterion has been obtained by requiring equilibrium of the section containing the flaw (Figure 7-1) when loads are applied. The detailed development is provided in Appendix A for a through-wall circumferential flaw in a pipe with internal pressure, axial force, and imposed bending moments. The limit moment for such a pipe is given by:

$$[\quad]^{a,c,e}$$

where:

[

]^{a,c,e}

The analytical model described above accurately accounts for the piping internal pressure as well as imposed axial force as they affect the limit moment. Good agreement was found between the analytical predictions and the experimental results (Reference 7-1). For application of the limit load methodology, the material, including consideration of the configuration, must have a sufficient ductility and ductile tearing resistance to sustain the limit load.

7.2 LOCAL FAILURE MECHANISM

The local mechanism of failure is primarily dominated by the crack tip behavior in terms of crack-tip blunting, initiation, extension and finally cracks instability. The local stability will be assumed if the crack does not initiate at all. It has been accepted that the initiation toughness measured in terms of J_{Ic} from a J-integral resistance curve is a material parameter defining the crack initiation. If, for a given load, the calculated J-integral value is shown to be less than the J_{Ic} of the material, then the crack will not initiate. Stability analysis using this approach is performed for selected location.

7.3 RESULTS OF CRACK STABILITY EVALUATION

A stability analysis based on limit load was performed. D.C. Cook Units 1 and 2 shop and field welds utilize SMAW and SAW weld processes. The "Z" factor for SMAW and SAW (References 7-2 and 7-3) are as follows:

$$Z = 1.15 [1.0 + 0.013 (OD-4)] \text{ for SMAW}$$

$$Z = 1.30 [1.0 + 0.010 (OD-4)] \text{ for SAW}$$

where OD is the outer diameter of the pipe in inches.

The Z-factors for the SMAW and SAW were calculated for the critical locations, using the pipe outer diameter (OD) of 10.75 inches. The applied faulted loads (Table 3-11 through Table 3-14 for Unit 1 and Table 3-15 through Table 3-18 for Unit 2) were increased by the Z factor. Material properties were used from Table 4-1. Table 7-1 summarizes the results of the stability analyses based on limit load for Unit 1 and 2. The leakage flaw sizes are also presented in the same table.

Additionally, elastic-plastic fracture mechanics (EPFM) J-integral analysis for through-wall circumferential crack in a cylinder is performed for select locations using the procedure in the EPRI Fracture Mechanics Handbook (Reference 7-4). Table 7-1 shows the results of this analysis.

7.4 REFERENCES

- 7-1 Kanninen, M. F., et. al., "Mechanical Fracture Predictions for Sensitized Stainless Steel Piping with Circumferential Cracks," EPRI NP-192, September 1976.
- 7-2 Standard Review Plan; Public Comment Solicited; 3.6.3 Leak-Before-Break Evaluation Procedures; Federal Register/Vol. 52, No. 167/Friday, August 28, 1987/Notices, pp. 32626-32633.
- 7-3 NUREG-0800 Revision 1, March 2007, Standard Review Plan: 3.6.3 Leak-Before-Break Evaluation Procedures.
- 7-4 Kumar, V., German, M.D. and Shih, C. P., "An Engineering Approach for Elastic-Plastic Fracture Analysis," EPRI Report NP-1931, Project 1237-1, Electric Power Research Institute, July 1981.

Segment	Pipe Size	Welding Process	Weld Location Node	Critical Flaw Size (in)	Leakage Flow Size (in)
I	10-inch	SMAW	2-SI-59-10-307	10.04	2.79
II	10-inch	SAW	2-SI-58-9-160Y	11.88	3.68
		SMAW	2-SI-58-9-162	12.32	3.64
		SAW	2-SI-58-6-184N	11.66	3.03
		SMAW	2-SI-58-6-184F	12.30	3.01
III	10-inch	SAW	2-SI-56-3-458F	18.34 ¹	9.17
		SMAW	2-SI-56-3-456	19.14 ¹	9.57

Note:

1. Calculated based on the methodology in Section 7.2

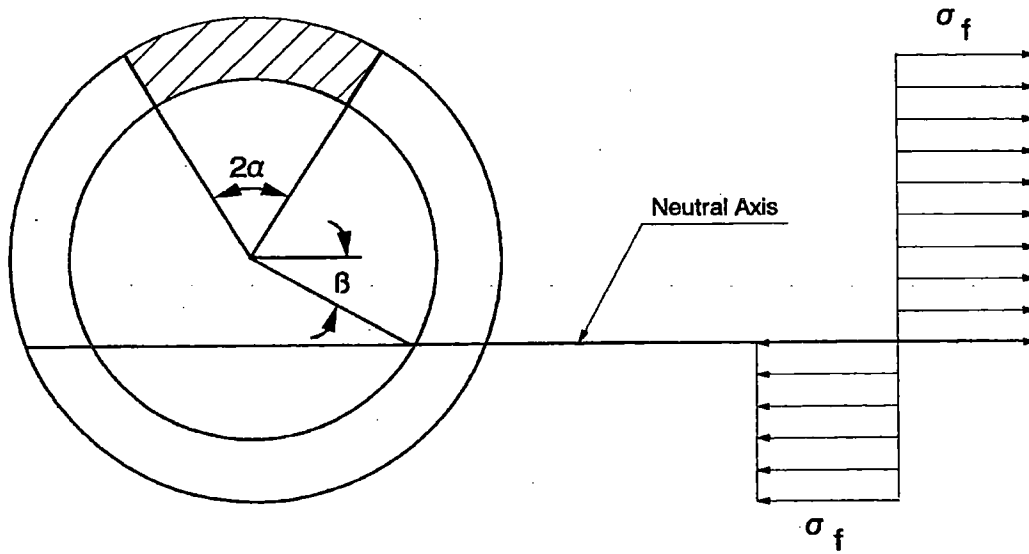


Figure 7-1 []^{a,c,e} Stress Distribution

8.0 ASSESSMENT OF FATIGUE CRACK GROWTH

The fatigue crack growth (FCG) analysis is not a requirement for the LBB analysis (see References 8-1 and 8-2) since the LBB analysis is based on the postulation of a through-wall flaw, whereas the FCG analysis is performed based on the surface flaw. In addition Reference 8-3 has indicated that, "the Commission deleted the fatigue crack growth analysis in the proposed rule. This requirement was found to be unnecessary because it was bounded by the crack stability analysis."

Also, since the growth of a flaw which leaks 8 gpm would be expected to be minimal between the time that leakage reaches 8 gpm and the time that the plant would be shutdown; therefore, only a limited number of cycles would be expected to occur.

8.1 REFERENCES

- 8-1 Standard Review Plan; Public Comment Solicited; 3.6.3 Leak-Before-Break Evaluation Procedures; Federal Register/Vol. 52, No. 167/Friday, August 28, 1987/Notices, pp. 32626-32633.
- 8-2 NUREG-0800 Revision 1, March 2007, Standard Review Plan: 3.6.3 Leak-Before-Break Evaluation Procedures.
- 8-3 Nuclear Regulatory Commission, 10 CFR 50, Modification of General Design Criteria 4 Requirements for Protection Against Dynamic Effects of Postulated Pipe Ruptures, Final Rule, Federal Register/Vol. 52, No. 207/Tuesday, October 27, 1987/Rules and Regulations, pp. 41288-41295.

9.0 ASSESSMENT OF MARGINS

The results of the leak rates of Section 6.4 and the corresponding stability evaluations of Section 7.3 are used in performing the assessment of margins. Margins are shown in Table 9-1 for Unit 1 and 2. All the LBB recommended margins are satisfied.

In summary, margins at the critical locations relative to:

1. Flaw Size - Using faulted loads obtained by the absolute sum method, a margin of 2 or more exists between the critical flaw and the flaw having a leak rate of 8 gpm (the leakage flaw).
2. Leak Rate - A margin of 10 exists between the calculated leak rate from the leakage flaw and the plant leak detection capability of 0.8 gpm.
3. Loads - At the critical locations the leakage flaw was shown to be stable using the faulted loads obtained by the absolute sum method (i.e., a flaw twice the leakage flaw size is shown to be stable; hence the leakage flaw size is stable). A margin of 1 on loads using the absolute summation of faulted load combinations is satisfied.

Segment	Pipe Size	Welding Process	Weld Location Node	Critical Flaw Size (in)	Leakage Flaw Size (in)	Margin
ACC-I	10-inch	SMAW	2-SI-59-10-307	10.04	2.79	3.6
ACC-II	10-inch	SAW	2-SI-58-9-160Y	11.88	3.68	3.2
		SMAW	2-SI-58-9-162	12.32	3.64	3.4
		SAW	2-SI-58-6-184N	11.66	3.03	3.8
		SMAW	2-SI-58-6-184F	12.30	3.01	4.1
ACC-III	10-inch	SAW	2-SI-56-3-458F	18.34	9.17	>2.0 ¹
		SMAW	2-SI-56-3-456	19.14	9.57	>2.0 ¹

Notes:

1. Margin of 2.0 demonstrated based on the methodology in Section 7.2

10.0 CONCLUSIONS

This report justifies the elimination of accumulator lines break from the structural design basis for D.C. Cook Units 1 and 2 as follows:

- a. Stress corrosion cracking is precluded by use of fracture resistant materials in the piping system and controls on reactor coolant chemistry, temperature, pressure, and flow during normal operation.

Note: Alloy 82/182 welds do not exist at the D.C. Cook Units 1 and 2 accumulator lines.

- b. Water hammer should not occur in the accumulator line piping because of system design, testing, and operational considerations.
- c. The effects of low and high cycle fatigue on the integrity of the accumulator line piping are negligible.
- d. Ample margin exists between the leak rate of small stable flaws and the capability of the D.C. Cook Units 1 and 2 reactor coolant system pressure boundary leakage detection systems.
- e. Ample margin exists between the small stable flaw sizes of item (d) and larger stable flaws.
- f. Ample margin exists in the material properties used to demonstrate end-of-service life (fully aged) stability of the critical flaws.

For the critical locations, flaws are identified that will be stable because of the ample margins described in d, e, and f above.

Based on loading, pipe geometry, welding process, and material properties considerations, enveloping critical (governing) locations were determined at which Leak-Before-Break crack stability evaluations were made. Through-wall flaw sizes were postulated which would cause a leak at a rate of ten (10) times the leakage detection system capability of the plant. Large margins for such flaw sizes were demonstrated against flaw instability. Finally, fatigue crack growth assessment was shown not to be an issue for the accumulator line piping. Therefore, the Leak-Before-Break conditions and margins are satisfied for D.C. Cook Units 1 and 2 accumulator line piping. It is demonstrated that the dynamic effects of the pipe rupture resulting from postulated breaks in the accumulator line piping need not be considered in the structural design basis of D.C. Cook Units 1 and 2.

APPENDIX A: LIMIT MOMENT

[

] ^{a,c,e}

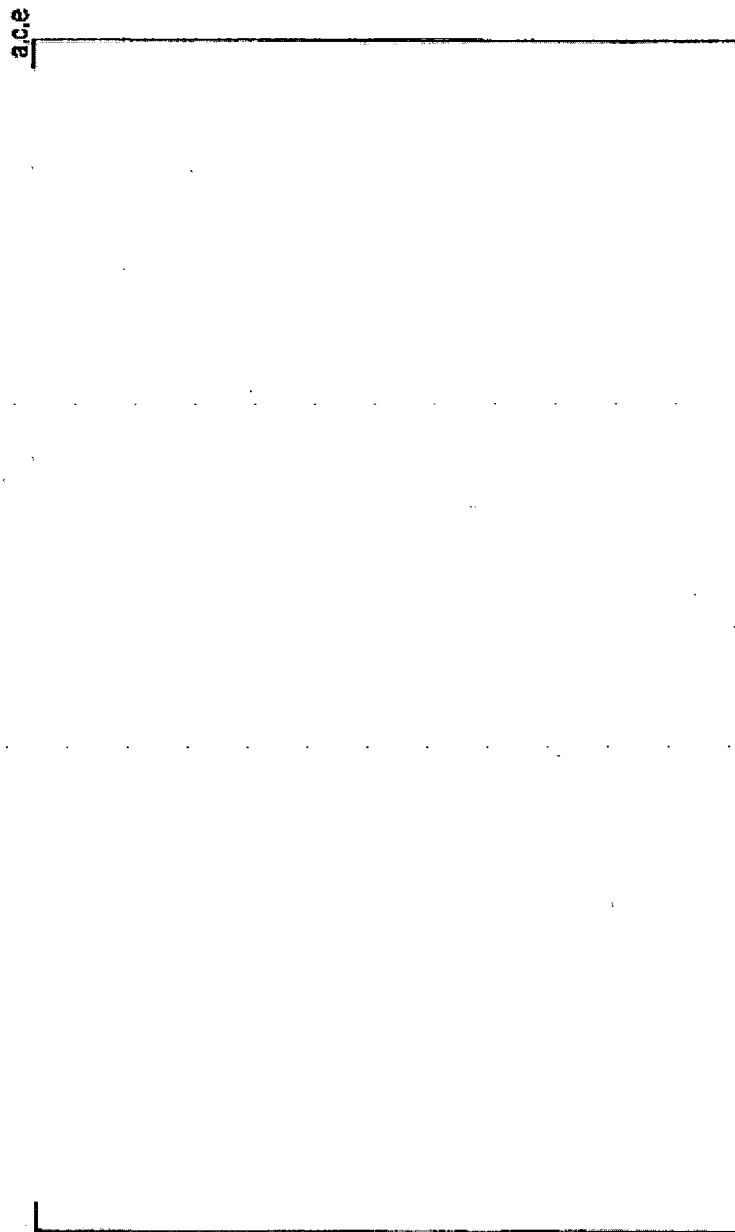


Figure A-1 Pipe with a Through-Wall Crack in Bending

This page was added to the quality record by the PRIME system upon its validation and shall not be considered in the page numbering of this document.

Approval Information

Author Approval Kirby Christopher R Jan-16-2018 14:21:34

Reviewer Approval Johnson Eric D Jan-17-2018 14:51:15

Manager Approval Leber Benjamin A Jan-18-2018 09:40:03

Files approved on Jan-18-2018

*** This record was final approved on 1/18/2018 9:40:03 AM. (This statement was added by the PRIME system upon its validation)